The Vertical Mass Transport from Troposphere to Stratosphere of an Indian Monsoon

by

BRENDA WYNETTA WALKER

B.S., Clark College
(1975)

Submitted in Partial Fulfillment
of the Requirements for the
Degree of

Master of Science

at the

Massachusetts Institute of Technology

(May, 1977)

Signature of Author.....
Department of Meteorology, May 12, 1977

Certified by.....
Thesis Supervisor

Accepted by.....
Chairman, Department Committee

The Vertical Mass Transport from Troposphere to Stratosphere of an Indian Monsoon

by

BRENDA WYNETTA WALKER

Submitted to the Department of Meteorology
on May 12, 1977 in partial fulfillment of the requirements
for the Degree of Master of Science

ABSTRACT

The tropospheric-stratospheric mass exchange processes have been investigated for a well-developed synoptic disturbance, the Indian Summer Monsoon. Vertical mass fluxes were examined for various triangular areas within the depression on the basis of mass balances.

Vertical motion was evaluated using the adiabatic thermodynamic equation, an approximate form of the diabatic thermodynamic equation and the continuity equation. Results using these three methods are critically compared. Absolute vorticity and rainfall distributions correlate satisfactorily with the calculated vertical velocity patterns.

The fluxes of mass and of the fluorocarbons $CFCl_3$ and CF_2Cl_2 across the tropopause have been estimated using vertical velocities obtained by the continuity equation and the diabatic thermodynamic equation. We find that over the three-day period 8/26/73 - 8/28/73 a mass of air equal to about 0.2% of the stratospheric mass was transported upwards through the 100 mb surface in an area of 10^6 km^2 in Northeastern India. Estimates

for the entire Indian Summer Monsoon were also made and indicate that the monsoons may be very significant in tropospheric-stratospheric exchange.

Name and Title of Thesis Supervisor:

Ronald G. Prinn

Associate Professor of Meteorology

CONTENTS

LIST OF FIGURES

ACKNOWLEDGMENTS

I am indebted to Professor Ronald Prinn for offering helpful discussions and assistance during this research work, and examining the rough draft of this paper. Thanks are extended to Drs. Fred Alyea and Derek Cunnold for introducing me to this research, as well as offering their guidance throughout this study, Mr. Steven Ricci for his assistance in drafting the figures, and Ms. Cheri Pierce for typing the final draft.

This work was supported by NASA Grants NSG-2196 and NSG-2010.

CHAPTER I

Introduction

Meteorologists have devoted considerable attention to the structure and motion fields of the upper troposphere and lower stratosphere.

The troposphere contains most of the mass and energy in the atmosphere and it is primarily the energy transformations in the troposphere which are responsible for our weather. However, the circulation of the stratosphere must be interrelated. The dynamics of the lower stratosphere are controlled by the tropospheric circulation and the tropospheric and stratospheric circulations govern the mass transport processes across the tropopause. The distribution of certain atmospheric constituents provides strong evidence of these exchange processes.

Reiter (1975) has stated, "the processes responsible for stratospheric-tropospheric mass exchange are: 1) seasonal variation of the mean tropopause level; 2) large-scale quasi-horizontal and vertical motions through the Hadley cell; 3) large-scale eddy transport; and 4) mesoscale and small-scale eddy transport across the tropopause."

Riehl and Malkus (1958) have pointed out that the upward flux in the Hadley cell in the lower troposphere does not occur as a continuous slow motion. It is necessary for mass and energy to be transformed from low levels to the high troposphere in the equatorial zone because observations show the strongest poleward mass flow and heat transfer in the Hadley cell takes place near the 200 mb level.

Riehl and Malkus demonstrate that in the higher levels it is necessary that the vertical transfer be accomplished by eddy motions rather than zonal mean motion. They concluded that the agent for this transport is updrafts concentrated in narrow "hot towers" of cumulus convection. These towers occasionally penetrate the tropopause and transport tropospheric air into the stratosphere. On the basis of the heat budget of the equatorial zone, they estimated that these "protected cores" occupy one-thousandth the area of the equatorial belt. Though the area covered by cumulus clouds in the tropics is large, it is the relatively rare high level cumuli which transport mass to the high troposphere and across the tropopause.

Satellite radiation analyses by Saha (1966), demonstrate that in southeast Asia high convective cumulonimbus clouds are observed over the land areas especially when synoptic disturbances are present. Thus, the synoptic disturbances can presumably transport mass up to various heights in the upper troposphere in these regions.

The purpose of this study is to quantitatively evaluate vertical fluxes of mass across the tropopause into the stratosphere by synoptic-scale disturbances. To accomplish this task the particular situation chosen to represent a strong and well developed synoptic disturbance was the Afro-Asian Monsoon.

The region extending from West Africa (30°W) eastward into the West Pacific (170°E) and between 35°N and 25°S experiences a marked seasonal shift of air currents called the monsoon. Ramage (1971) defined the monsoon areas as "... encompassing regions with January and July surface circulations in which:

1) the prevailing wind direction shifts by at least 120° between January and July,

2) the average frequency of prevailing wind directions in January and July exceeds 10%,

3) the mean resultant winds in at least one of the months exceed 3 ms^{-1}, and

4) fewer than one cyclone-anticyclone alternation occurs every two years in either month in a 5° latitude-longitude rectangle".

In the present study the specific case in question is the 1973 Indian Summer Monsoon. By employing the dynamic constraints of continuity and thermodynamics, mass transport processes from troposphere to stratosphere were investigated. Chapter 2 outlines the synoptic structure of the monsoon circulations. In Chapter 3 the data sources and the methods used to calculate the large-scale vertical motion are discussed. Krishnamurti (1975) has found there is large vertical motion over the monsoon region if one uses the continuity equation to calculate vertical velocities in a monsoon depression. A comparison between the vertical velocities computed using the continuity equation and the first law of thermodynamics is made. Chapter 4 deals with the distribution of rainfall, vertical motion and absolute vorticity. Chapter 5 evaluates the vertical flux of mass and fluorocarbons across the tropopause. The final summary chapter emphasizes the impact of our results on tropospheric-stratospheric exchange processes.

CHAPTER 2

Monsoon Circulations

2.1 Regional Climatology

It is observed that during the northern summer an extensive low pressure area persists between North Africa and East China and from 30°N to 10°S, displacing the upward branch of the Hadley cell to north of the Himalayas. The southeasterly trade winds of the southern hemisphere which cross the equator under the influence of the thermal force of the Hadley cell and turn into a southwesterly current are referred to as the "southwest monsoon".

The vertical structure of the circulation is characterized by lower tropospheric westerlies and upper tropospheric easterlies.

One of the most fascinating features of the monsoon system is the tropospheric tropical easterly jet near 200 mb. This jet has winds of roughly 19 ms^{-1} - 50 ms^{-1}. The first comprehensive study of the Tropical Easterly Jet over Asia was done by Koteswaram (1958). He found that the jet center occurs near 15°N and that the current accelerates east of 75°E and decelerates west of 75°E. Flohn's (1964) study has indicated that the jet is located near 150 mb with maximum winds of 30 ms^{-1}. The observational aspects of this jet have been modeled by Murakami, et al. (1970). This model has simulated many of the known broad-scale features of the monsoon. Some of these are:

i) southwest monsoon flows in the lower troposphere below 600 mb north of the equator

ii) warm upper troposphere between 10°N and 30°N

iii) an anticyclone near 25°-30°N at 200 mb

iv) a pronounced easterly jet; speeds of 17-20 ms^{-1} near 150 mb (14 km)

v) a local Hadley cell with an ascending branch near 20°N and a descending branch near 3°S

Although the monsoon is one system, three dissimilar regional circulations exist:

i) west of 70°E: middle troposphere subsidence, large vertical wind shear

ii) between 70-105°E: large scale upward motion, large vertical wind shear, monsoon depressions, subtropical cyclones, and frequent rains.

iii) east of 105°E: intermittent upward motion, small vertical wind shear, typhoons, subtropical cyclones and changeable weather.

2.2 Indian Monsoon Depression

In the summer the surface pressure trough or "monsoon trough" over the Indian subcontinent is oriented northwest - southwest, lying to the south of and roughly paralleling the Himalayas. The eastern end of the trough over the northern Bay of Bengal is the birthplace of the depression.

Koteswaram and Rao (1963), contended that a monsoon depression develops when a low pressure wave moves from Burma to the northern Bay of Bengal. Of four or five low pressure waves which move into the Bay of Bengal during an average summer monsoon month, two or three intensify into a monsoon depression.

Monsoon depressions move as tropical cyclones do, west-northwestward. Central pressures range from 2-10 mb below normal. Monsoon depressions appear weak yet they often persist for a week or more over

land giving widespread and frequent rains.

The vertical structure of the circulation is characterized by lower tropospheric westerlies, which attain a maximum speed of 7-10 ms^{-1} at about 850 mb and upper tropospheric easterlies which attain a maximum speed of 20-30 ms^{-1} at about 150 mb. The transition from lower level westerlies to upper level easterlies occurs at about 500 mb. Figures 1 and 2 show the mean zonal flow for the Indian continent for the month of August, 1973 at 80°E and 77°E. Figure 3 shows the cross-section of potential temperature. Examining Figures 1, 2, and 3 it can be seen that the vertical structure of the mean circulation is fairly homogeneous at low latitudes.

Figures 4-6 show the monsoon depression located over northeast India on the 26th of August through the 28th of August, 1973. Krishnamurti (1975) states that

> "The horizontal scale of the depression is about 2,000 km, the vertical scale about 10 km, its westward speed of motion about 5° longitude/day. The monsoon depression is an intense close vortex that has horizontal wind speeds of about 10-15 mps and its closed circulation extends to about 9 km in the vertical ... Vertical motions show rising motion west of, i.e., ahead of, the trough line and descending motion to the rear...".

These statements were made in reference to a detailed analysis of the structure of a monsoon depression.

Shukla contends it is unclear why the authors considered the horizontal scale of the depression as 2,000 km. He concludes that it would seem more reasonable to take 3,000 km for this scale. Here we have implicitly assumed a horizontal scale of 2,000-3,000 km but the exact value is not an important factor in our analysis.

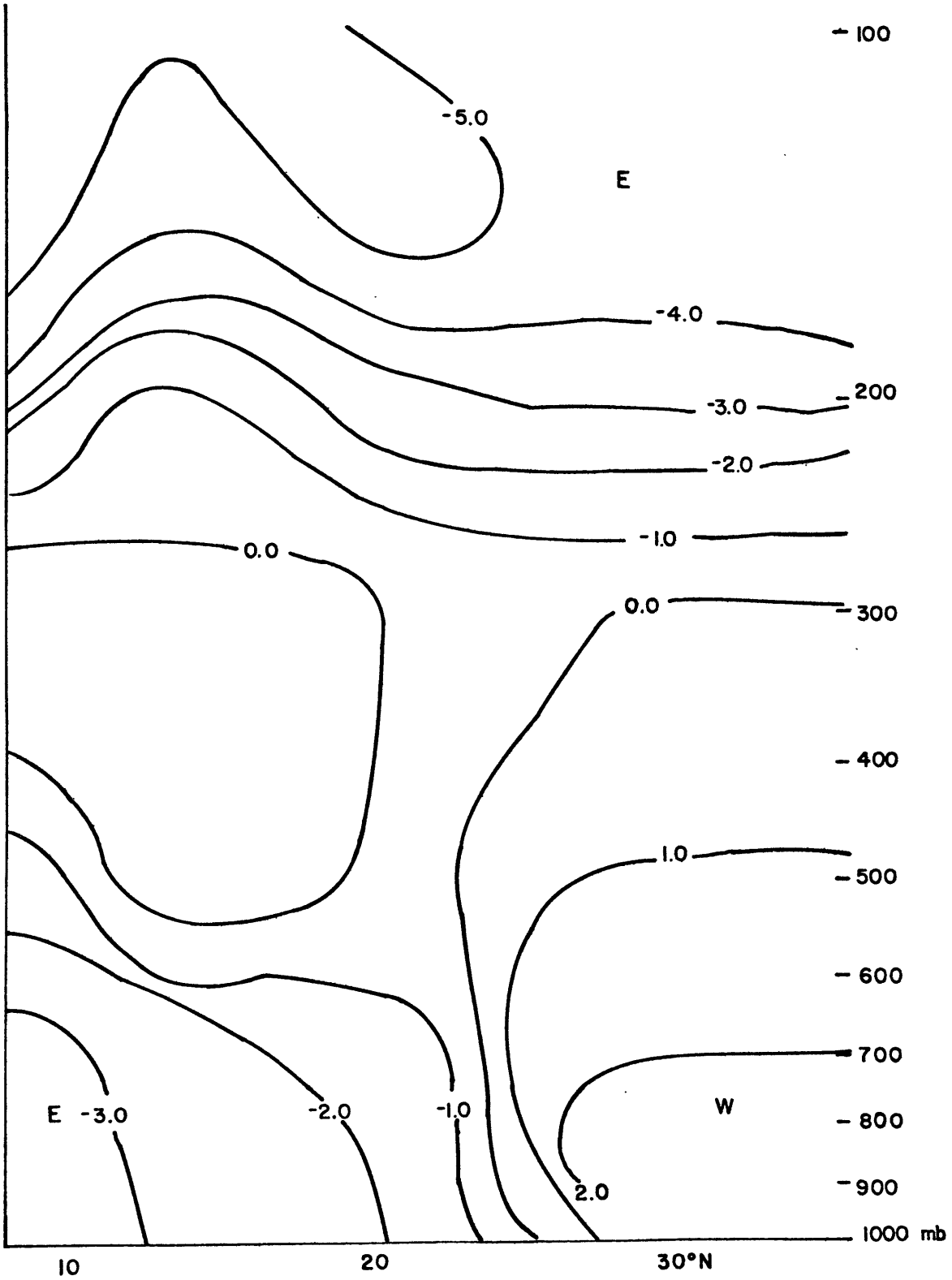

Figure 1. Mean zonal flow along 80°E for August, 1973.
Wind speed in m/s.

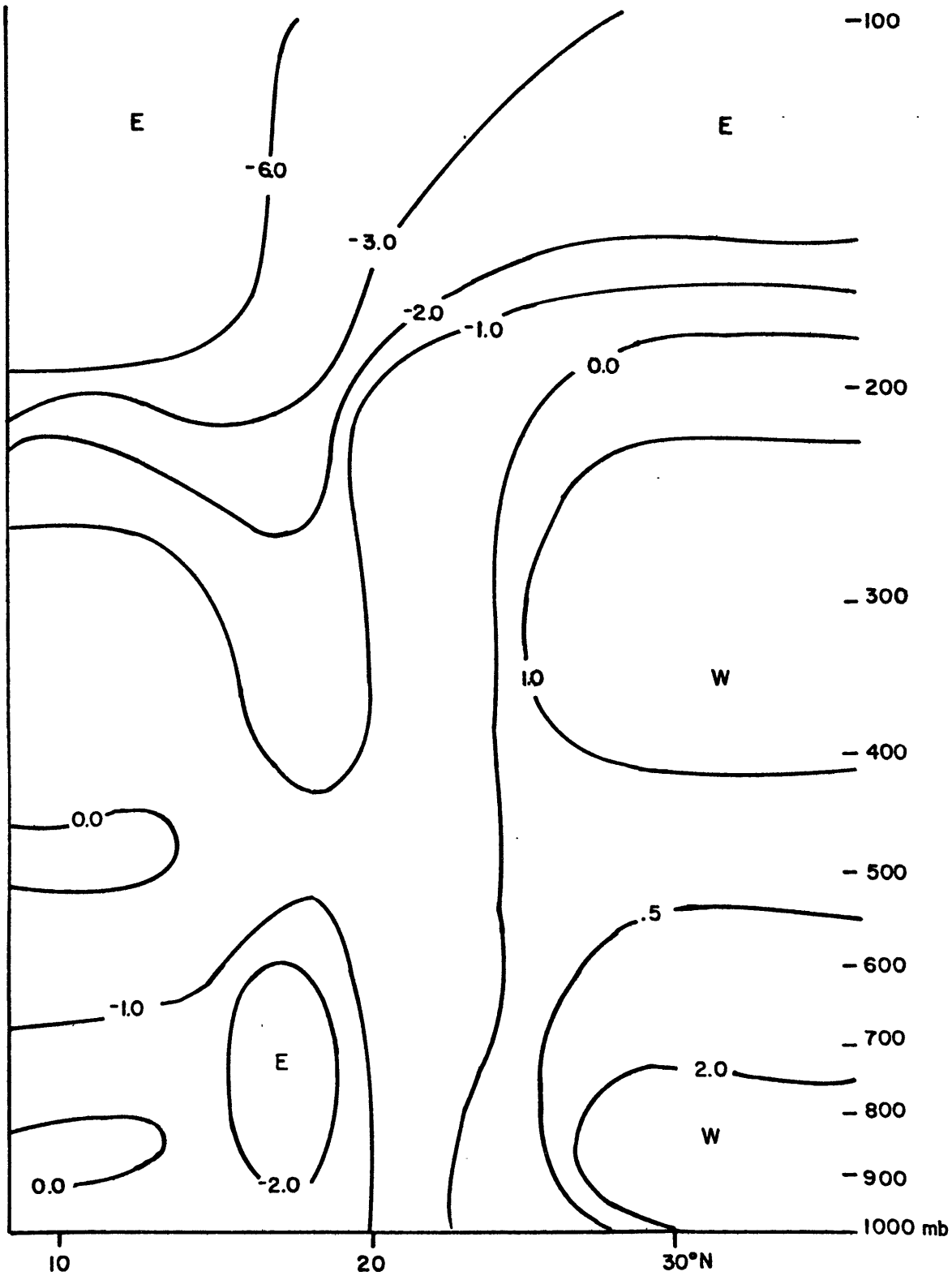

Figure 2. Mean zonal flow along 77°E for August, 1973.
Wind speed in m/s.

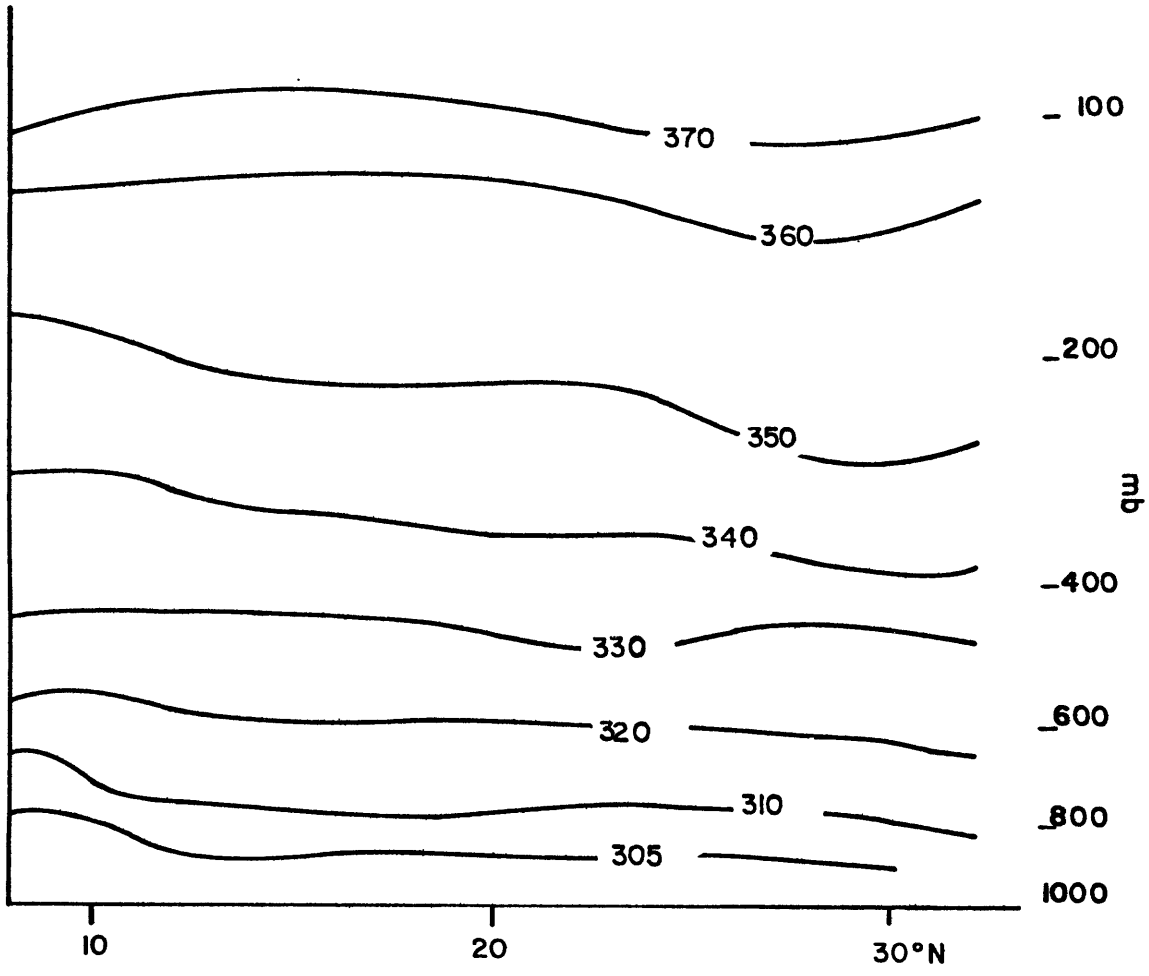

Figure 3. Vertical cross-section of potential temperature along the 80°E meridian. Temperature in °K.

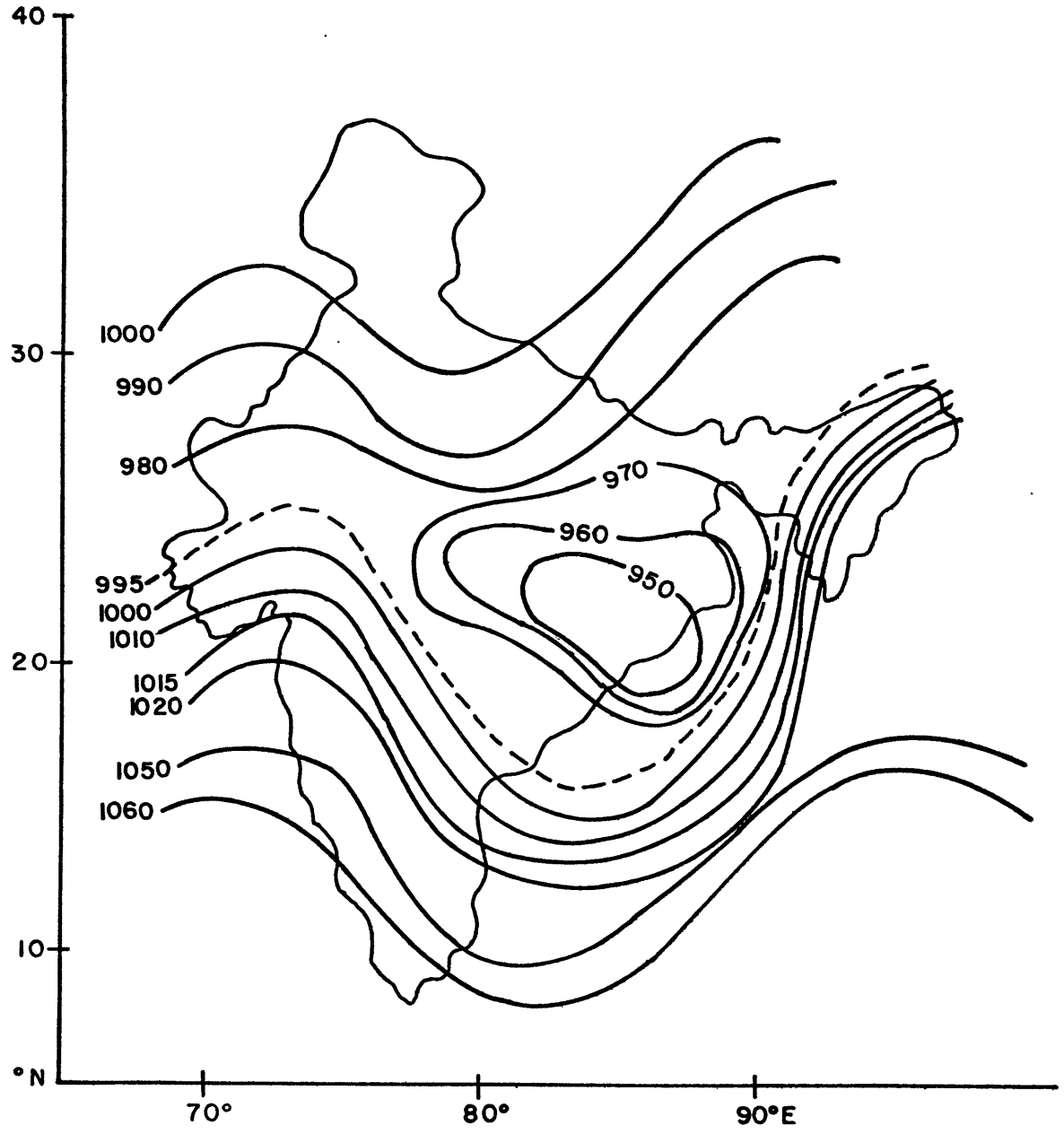

Figure 4. Surface pressure map (mb) for 12Z, August 26, 1973.

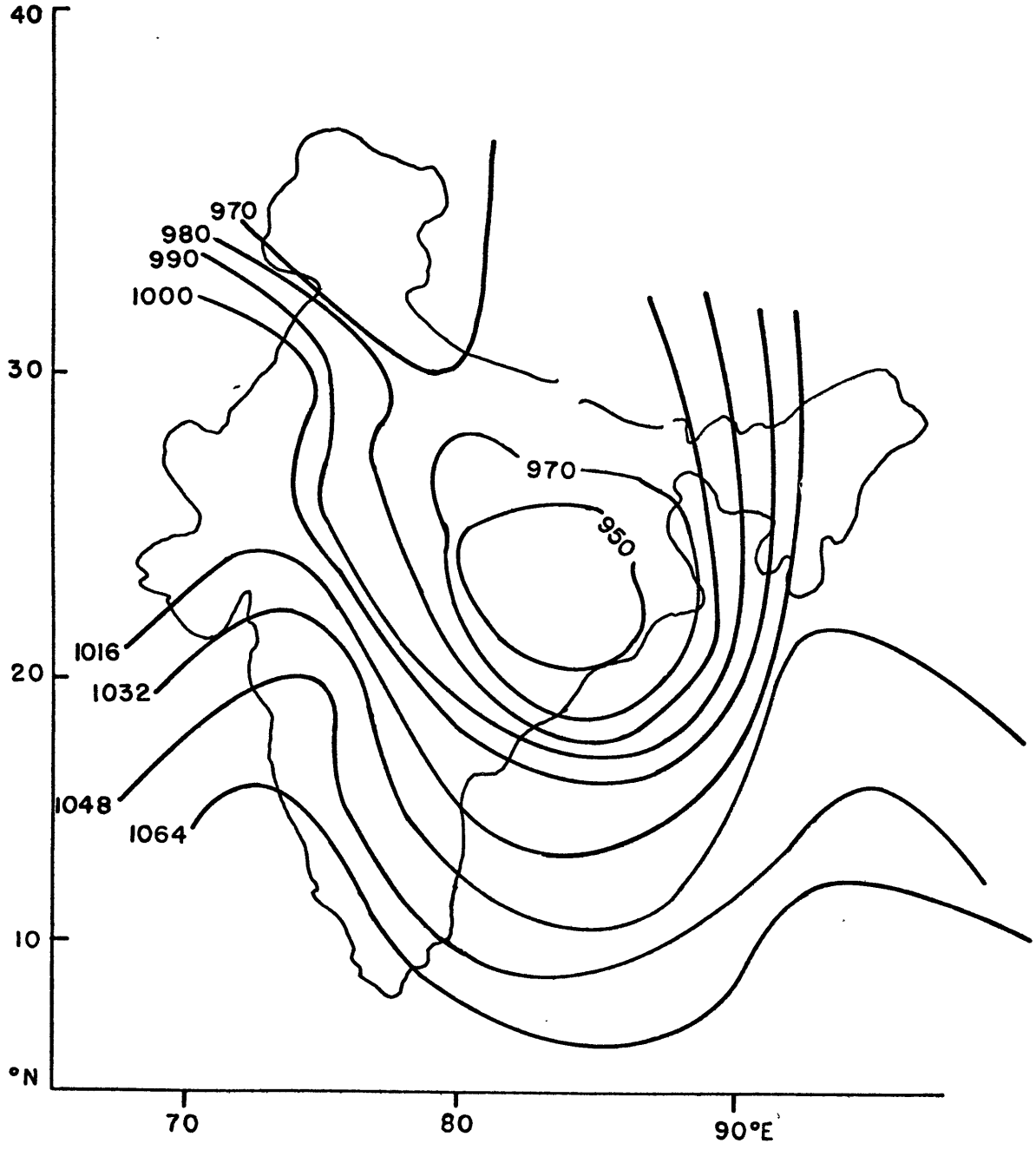

Figure 5. Surface pressure map (mb) for 12Z, August 27, 1973.

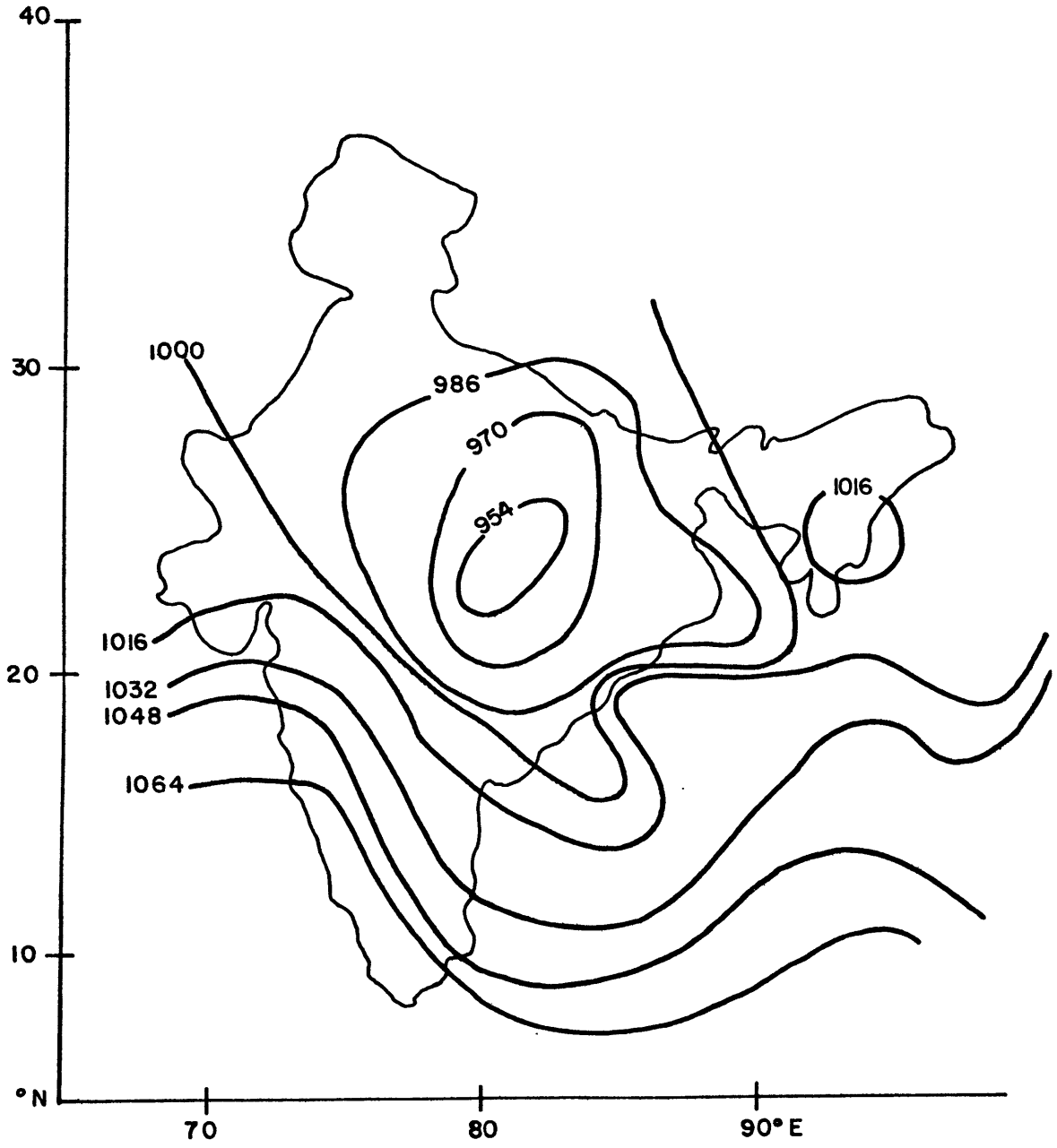

Figure 6. Surface pressure map (mb) for 12Z, August 28, 1973.

CHAPTER 3

Computation of Large-Scale Vertical Motion

3.1 Data

Most data used in this study were obtained from the National Center for Atmospheric Research. Radiosonde and surface observations were analyzed for six Indian stations (Table 1) between August 26 through August 28, 1973 inclusive. The principal reporting time was 1200 GMT.

Our approach for studying the transport processes was to utilize temperature, pressure, wind direction and velocities observed for twenty levels in 50 mb intervals from 1000 mb to 50 mb. The thermal wind equation was utilized to check the station analysis of the observed wind and temperature fields for consistency. At each of the twenty levels divergences were computed by the Bellamy (1949) method for various combinations of triangular areas from the six stations chosen. Figure 7 shows the smaller triangles for which divergences were computed. The average cross-sectional area of these triangles is 2.5×10^5 km^2. Figure 8 shows the large triangles for which divergences were computed. The average cross-sectional area of these triangles is 4.0×10^5 km^2. Vertical motions were then inferred from the divergences computed.

Vertical and horizontal cross-sections were drawn for the vertical motion, rainfall distribution and the absolute vorticity for the Indian region between 15°N and 30°N and between 75°E and 85°E.

The disturbance studied formed over the Bay of Bengal around the 25th of August, 1973. Figures 4, 5, and 6 illustrate the surface

TABLE 1

WMO #	STATION
42182	NEW DELHI
42339	JODHPUR
42369	LUCKNOW/ AMAUSI
42809	CALCUTTA
42867	NAGPUR
43149	VISHAKHAPATNAM

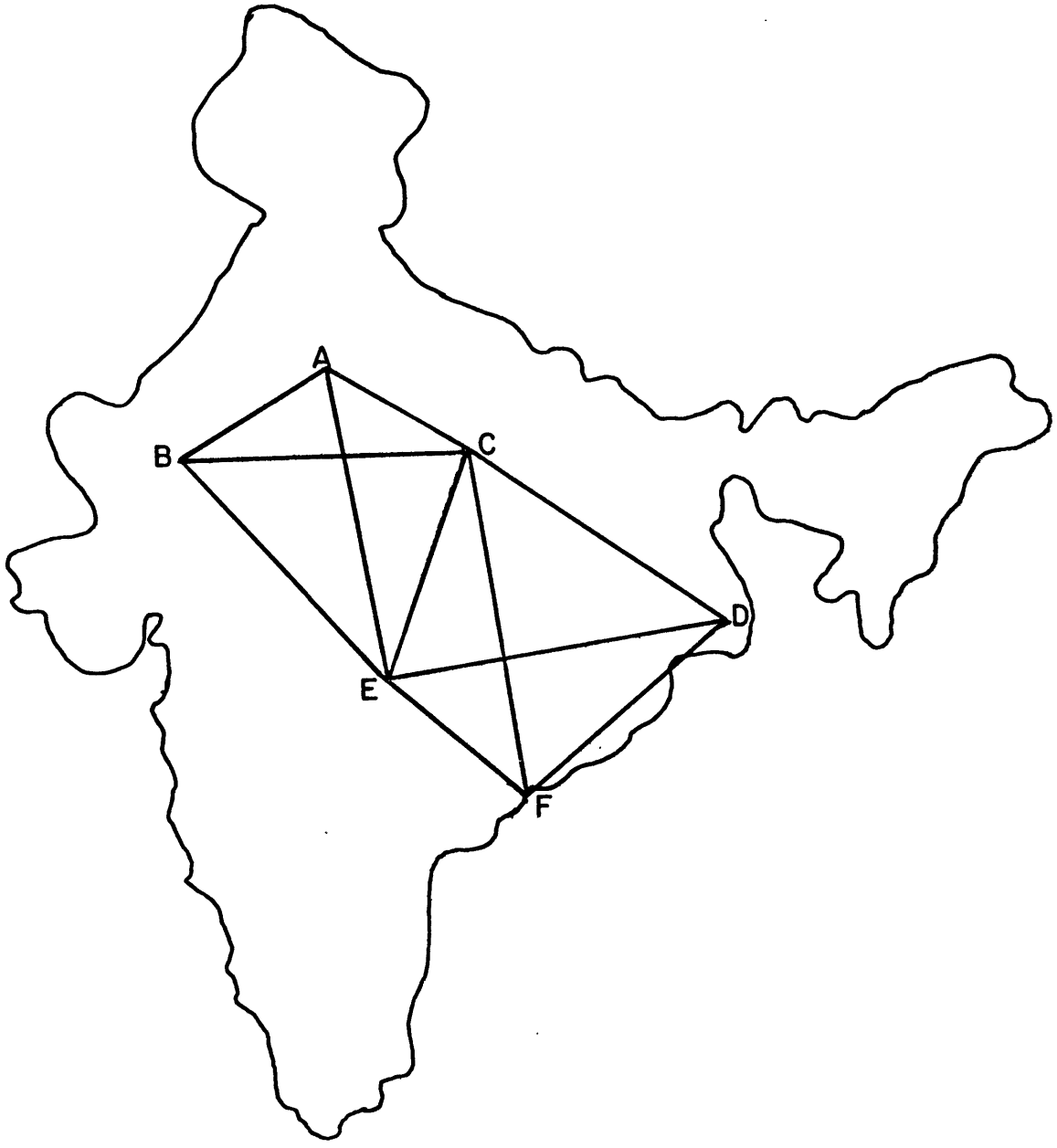

Figure 7. Vertical velocities computed for triangles ABC, BCE, ABE, AEC, CEF, CFD, CED, DEF.

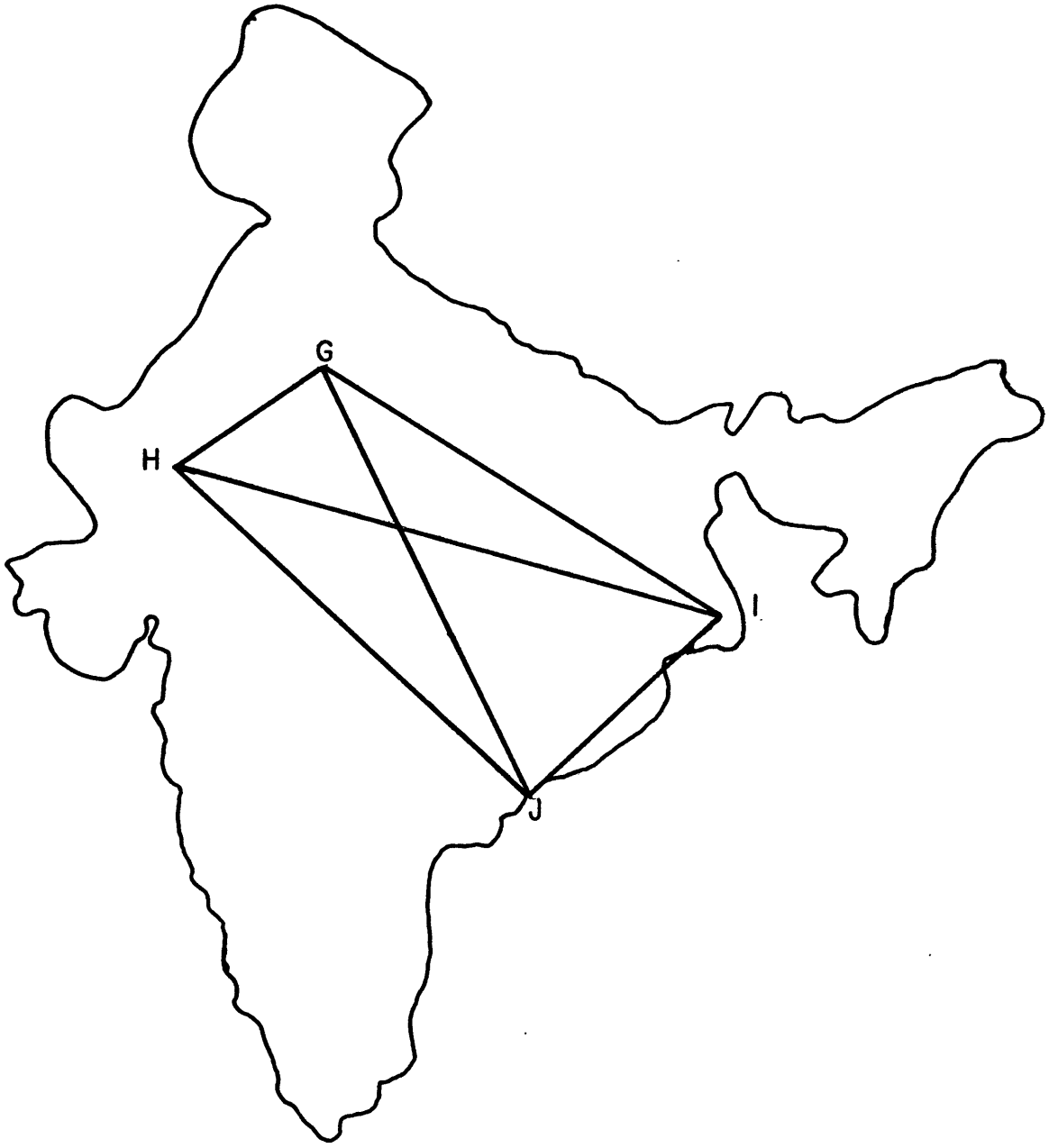

Figure 8. Vertical velocities computed for triangles HIJ, GIJ, GHJ, GHI.

pressure field for the sequence of three days. The depression has a central pressure of around 950 mb and propagates westward with a speed of approximately 3° longitude/day. The total rainfall was an average of approximately 13.7 cm for the northeastern area over the three days.

The atmospheric large scale motion is nearly horizontal and the vertical velocity is too small to measure directly. However, the vertical velocity governs the rate of condensation and precipitation which has a large influence on the general circulation in the tropical regions.

There are several methods for calculating the vertical velocity; the two methods employed in this study were the use of the continuity equation (i.e., kinematic method) and the First Law of Thermodynamics. The accuracy of these particular methods and indeed of any other method depends on the quality and quantity of available data. The purpose of this chapter is to describe the methods by which the large-scale vertical velocity has been computed for use in our study.

3.2 The First Law of Thermodynamics

Changes in the atmosphere are governed by the laws of physics which can be expressed in the form of certain differential equations. From the first law of thermodynamics

$$C_p \frac{I}{\theta} \frac{d\theta}{dt} = Q \qquad (3.1)$$

where Q is the net heating, including solar heat, latent heat release turbulent transfer of sensible heat at the boundary layer and infrared cooling.

Further expansion of 3.1 yields

$$\frac{\partial \theta}{\partial t} + V \cdot \nabla_H \theta + \omega \frac{\partial \theta}{\partial p} = \frac{\theta Q}{C_p T} \qquad (3.2)$$

The adiabatic thermodynamic equation

$$\frac{\partial \theta}{\partial t} + V \cdot \nabla_H \theta + \omega \frac{\partial \theta}{\partial p} = 0 \qquad (3.3)$$

was applied to calculate vertical velocities for 9 triangular regions covering the northeastern India area from 1000 mb to 50 mb in 50 mb intervals.

Figures 12-18 show the distribution of the vertical velocities calculated from Equation 3.3 in some of the small triangles for two of the three days investigated. It should be noted that in many of the illustrations the lower layers indicate weak descending motion. Since the latent heating is ignored the adiabatic thermodynamic equation is however invalid in all precipitating regions. The average maximum height of cloud tops observed in the region was 5 km. Therefore the adiabatic thermodynamic equation is expected to be invalid below the 400 mb level. Above this level Figures 12, 14, and 17 indicate net downward motion for August 27, August 27, and August 28, respectively. Figures 13, 15, 16, and 18 indicate ascending motion above this level except for apparent subsidence at the uppermost levels. Figures 21 and 22 show the distribution of vertical velocity in one of the large triangles studied. There is net descending motion observed on August 27 (Figure 21), and net ascending motion from 400 mb to 175 mb on August 28 (Figure 22).

In the absence of precipitation, vertical motion is expected to be small. For precipitating systems the latent heating must be incorporated. Each term in Equation 3.2 was calculated for the twenty surface levels for each of our six Indian stations over the 3 days investigated. Comparing the magnitudes of these terms we found the following characteristic scales:

$$\frac{d\theta}{dt} \sim 10^{-5} \quad ds^{-1}$$

$$V \cdot \nabla\theta \sim 10^{-6} \quad ds^{-1}$$

$$\frac{\partial\theta}{\partial p} \sim 10^{-2} \quad dmb^{-1}$$

$$\frac{\theta Q}{C_p T} \sim 10^{-3} \quad ds^{-1}$$

Note that the $\omega \partial\theta/\partial p$ term dominates the left-hand side of Equation 3.2 provided $\omega > 10^{-3}$ mbs^{-1}. Under these circumstances Equation 3.2 can be approximated by

$$\omega \frac{d\theta}{dp} = \frac{\theta Q}{C_p T} \tag{3.4}$$

Surface data were analyzed and the average rainfall rates over the three-day period for the triangular areas were estimated. However, in attempting to find the daily rainfall in our triangular areas alone we found the data too inconsistent for an accurate analysis. Therefore the daily rainfall for the entire northeastern region was determined. The average heating rate per unit mass of air can thus be calculated providing we take into account the fact that the condensation due to the convective clouds is not distributed evenly over the entire vertical column. For this latter purpose the vertical profile for Q, given by Yanai et al.

(1973), was used as an estimate of the distribution of non-radiative diabatic heating (Figure 19). We were cognizant of the fact that this distribution is not characteristic of all tropical systems. However, it is an indication of the heating distribution provided by moist convection processes.

The average daily rainfall for the northeast region was 4.4 cm for August 26, 3.3 cm for August 27, and 5.0 cm for August 28. These rainfall amounts and Equation 3.4 yield vertical velocities of 1.0×10^{-3}, 8.0×10^{-4} and 1.2×10^{-3} mbs^{-1} for the three days respectively at the 100 mb level. These values are applied over an area of 9.5×10^{5} km^2.

The average total rainfall for a triangular area of 6.5×10^{5} km^2 for the three days was 13.7 cm. Figure 23 shows the average vertical velocity distribution using Equation 3.4 up until the 100 mb surface. The largest magnitudes are on the order of 1.5×10^{-2} mbs^{-1}. Vertical velocities reach a maximum at the 300 mb level. The vertical velocity observed at the 100 mb level is 3.2×10^{-3} mbs^{-1}.

The values of the vertical velocities computed using Equation 3.4 are consistently 2 orders of magnitude larger than the average vertical velocities calculated using Equation 3.3 and occasionally one order larger than the velocities calculated using the continuity equation even at the uppermost levels (see next section).

Figures 9, 15, 16, 18, and 20 show vertical velocities computed by the continuity equation for a number of triangles in which the maximum magnitude of their values is about 10^{-2} mbs^{-1}. The observed total precipitation in these particular cases was approximately 10 cm for the three days at some of the stations within these triangles. Note that the vertical velocities shown in Figure 23 are of the same magnitude as

the velocities computed by the continuity equation within these triangles.

The distribution of upward velocities is far from homogeneous and in particular the average vertical motion in the triangles with precipitating disturbances is usually an order of magnitude larger than the vertical motion outside of the disturbance. The sizes of these disturbances are therefore relevant. Satellite cloud observations were analyzed to determine the size of these storms but because of the widespread cloudiness in this region we were unable to make an estimate. Billa and Raj (1966) used a triangle of recording rain gauges near Poona (18°35', 73°55'E) to measure the dimensions of five mesoscale rain systems during the summer of 1964. The median radius was 55 km. Thus approximately 11% of the total area of a small triangle and 8.7% of the total area of a large triangle may be comprised of intense storms.

3.3 Vertical Velocities Calculated from the Continuity Equation

The average vertical velocity $\overline{\omega}$ in pressure coordinates was computed by integrating the continuity equation in the form,

$$\frac{\partial \overline{\omega}}{\partial p} = - \overline{\nabla_H \cdot V} \qquad (3.5)$$

where $\overline{\omega} = dp/dt$, $\overline{\nabla_H \cdot V}$ is the same mean divergence of the horizontal velocity vector v and p is pressure. The velocity divergence was computed by the Bellamy (1949) method for the triangle. When integrated over a layer from p_o to p_1 the vertical velocity at the top of the layer is given by

$$\bar{\omega}_1 = \bar{\omega}_0 + \overline{(\nabla_H \cdot V)}_{\frac{1}{2}}(p_0 - p_1) \tag{3.6}$$

where $\bar{\omega}_0$ is the vertical velocity at the bottom of the layer and $\overline{(\nabla_H \cdot V)}_{1/2}$ is the mean divergence between levels p_0 and p_1. It was assumed that $\bar{\omega}_0 = 0$ at 1000 mb and $\bar{\omega}$ was then computed in the 1000 mb to 50 mb region in 50 mb intervals.

Figures 9-18 and 20-23 show the distribution of the vertical velocities obtained by Equation 3.6. The average magnitude of the vertical velocities is 5×10^{-3} mbs^{-1}.

A comparison of the results of the two methods is of interest. The major difference is that the kinematic vertical velocity values are always larger than the vertical velocity values obtained by Equation 3.3. As stated in the previous section, the adiabatic thermodynamic equation 3.3 is assumed valid in the upper troposphere and invalid in the lower troposphere. It is also well known that the vertical velocities calculated by the kinematic method are highly sensitive to errors. These errors accumulate in the vertical integration of the mass continuity equation. However, it is plausible that the vertical velocities obtained in the lower layer are realistic because of the smaller number of errors expected to have accumulated. The level of maximum convergence is higher for the kinematic method. In general, the distribution of vertical motions obtained using Equations 3.3 and 3.6 correlate (see Figures 12-18 and 21-22).

Previous computations of the vertical velocities in the typical monsoon region indicate an area of ascending motion over northeast India

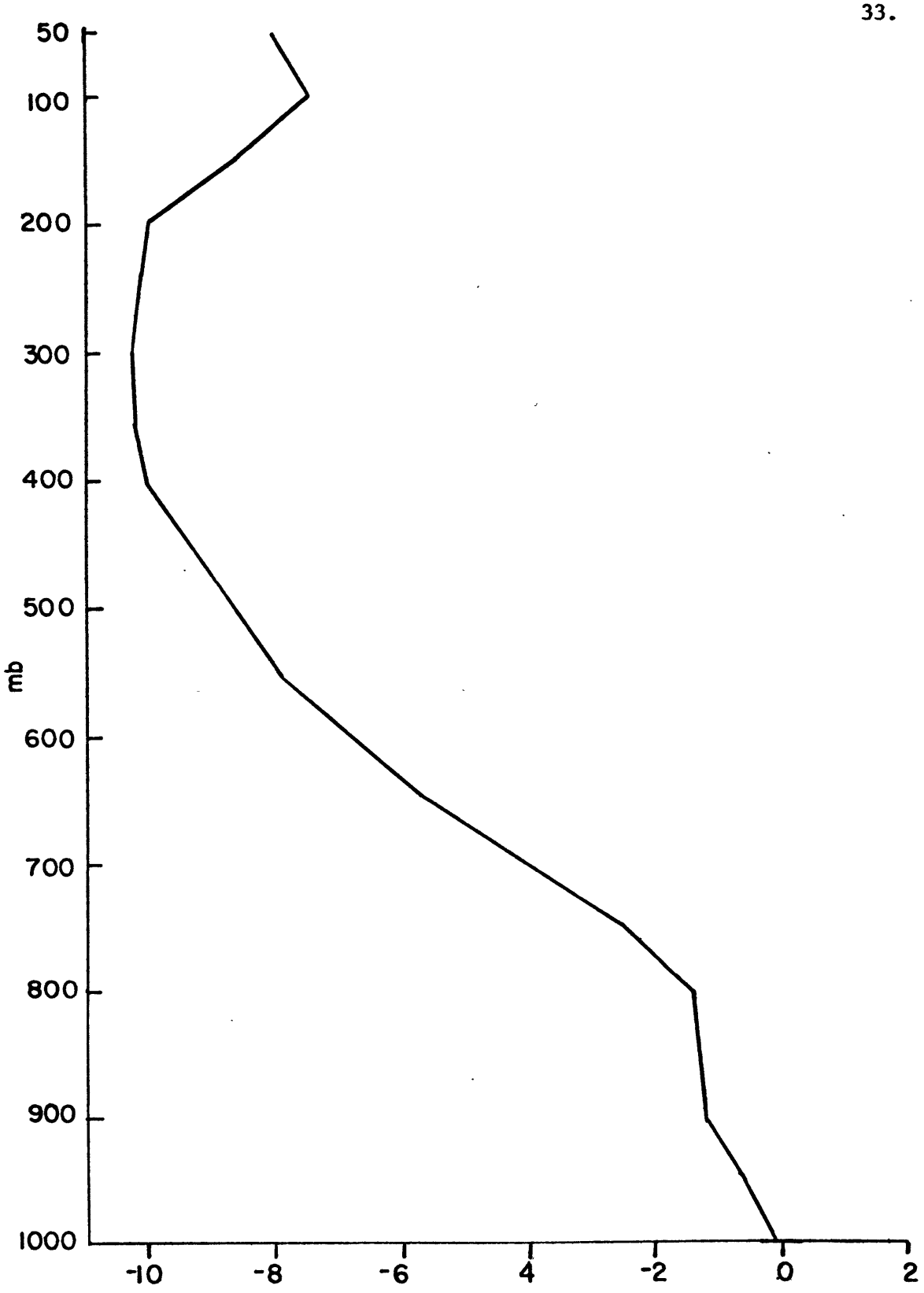

Figure 9. Distribution of vertical velocities (10^{-3}mb/s) for triangle DEF on August 26, 1973 calculated from the continuity equation.

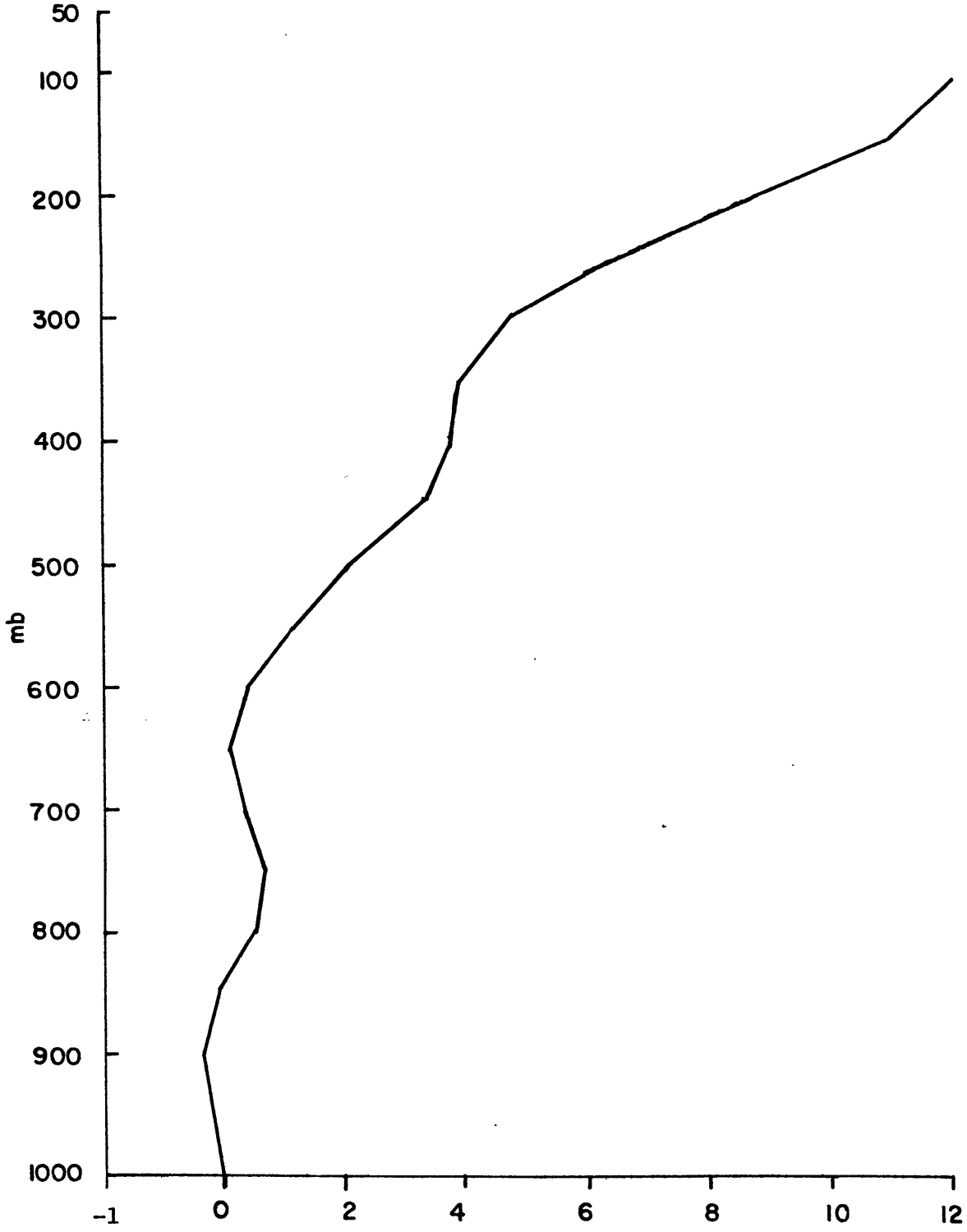

Figure 10. Distribution of vertical velocities (10^{-3} mb/s) calculated from the continuity equation for triangle CEF on August 26, 1973.

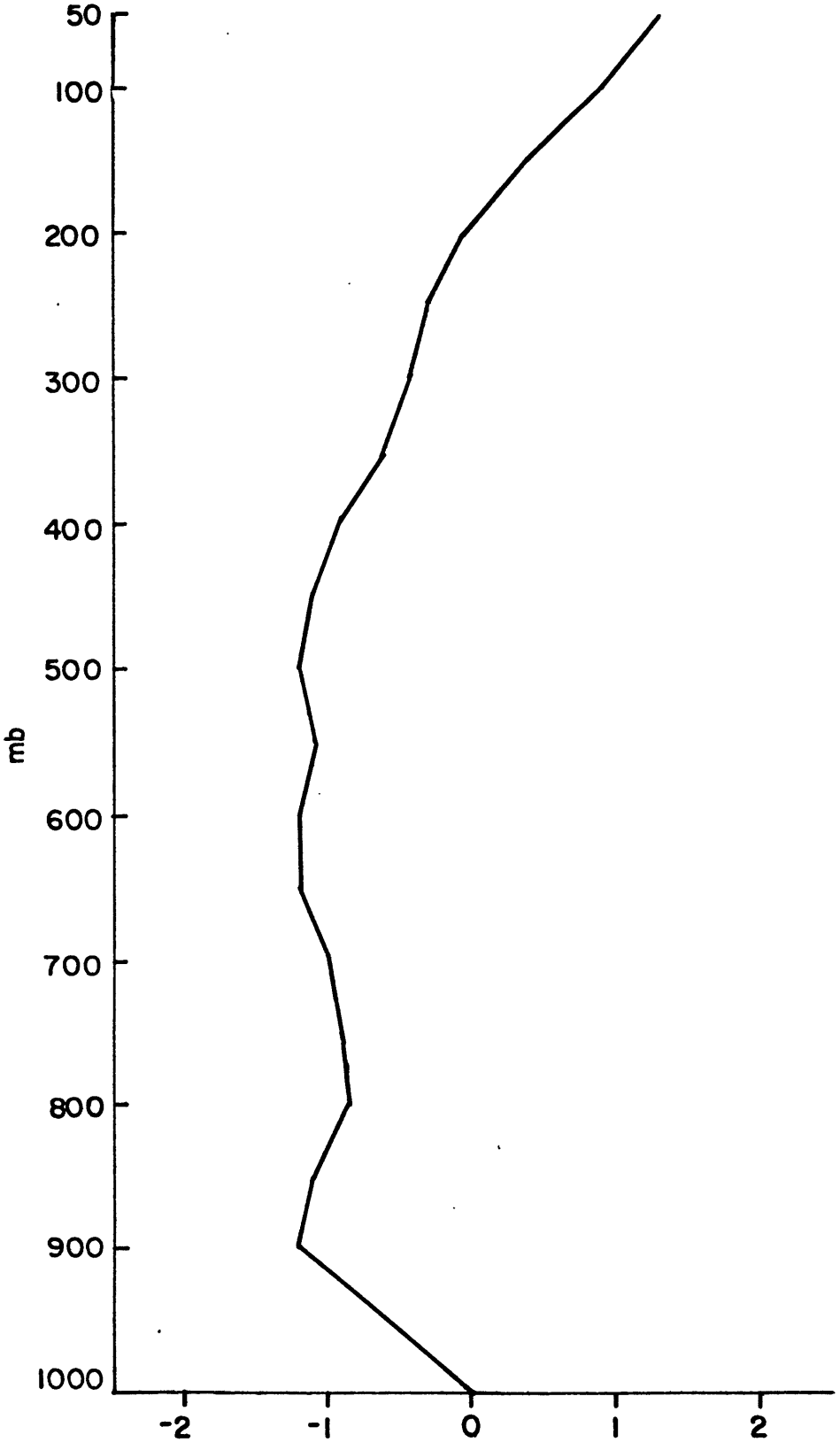

Figure 11. Distribution of vertical velocities (10^{-3} mb/s) calculated from the continuity equation for triangle CED on August 26, 1973.

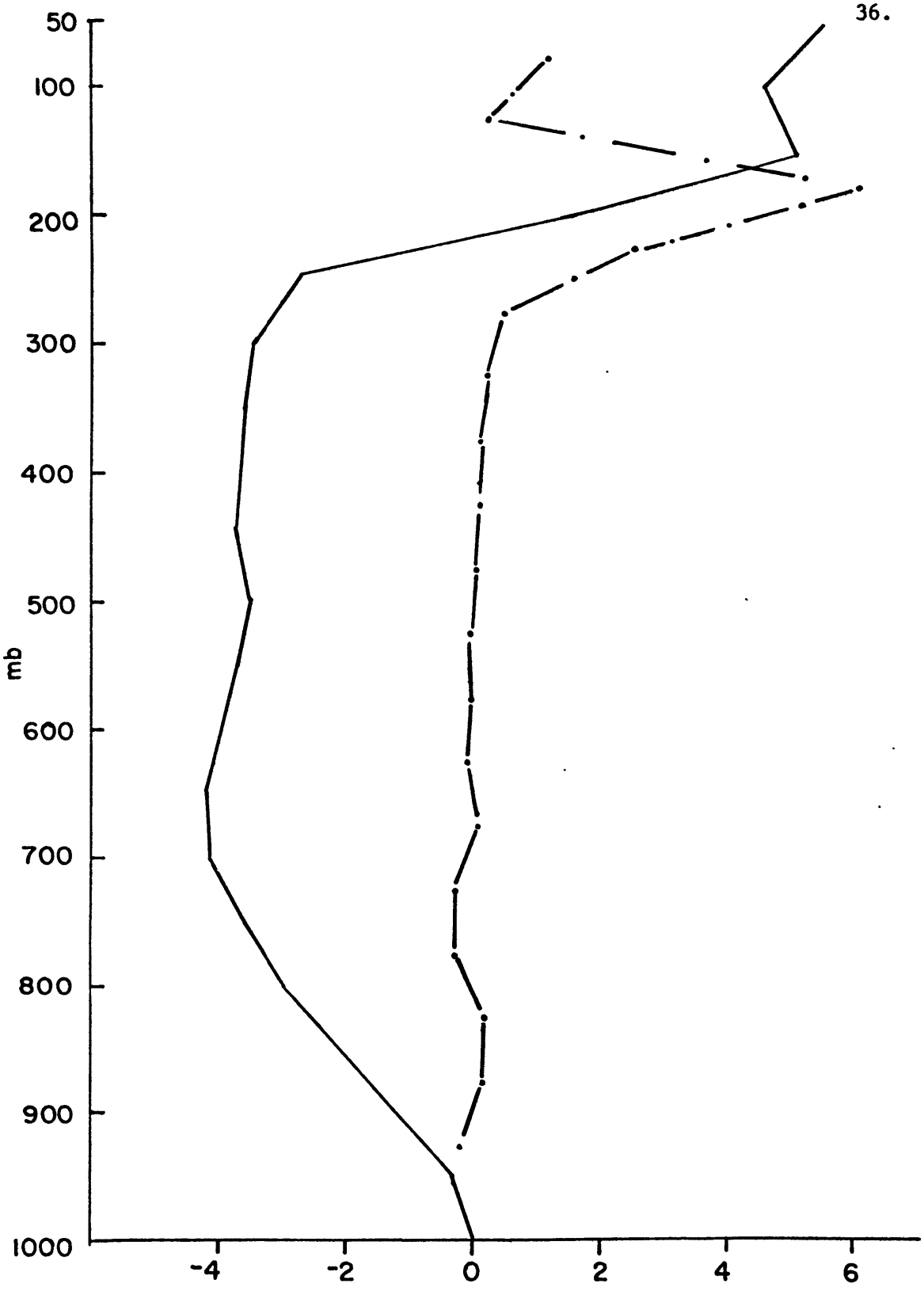

Figure 12. Distributions of vertical velocities calculated from the continuity equation (——) and the adiabatic thermodynamic equation (—·—·), (10^{-3} mb/s), for triangle DEF on August 27, 1973.

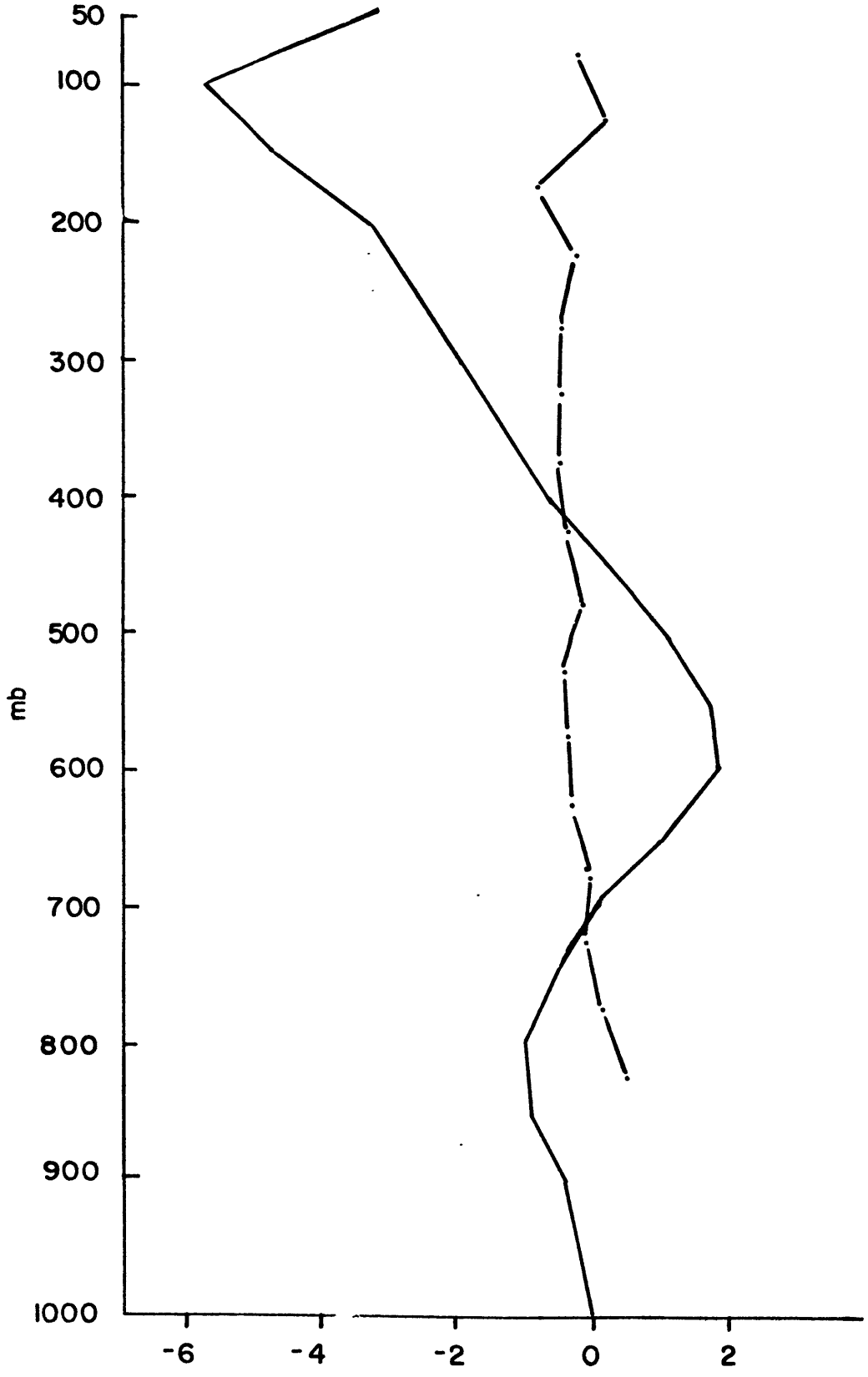

Figure 13. Distributions of vertical velocities (10^{-3} mb/s), calculated from the continuity equation (——) and the adiabatic thermodynamic equation (—·—·) for triangle CEF on August 27, 1973.

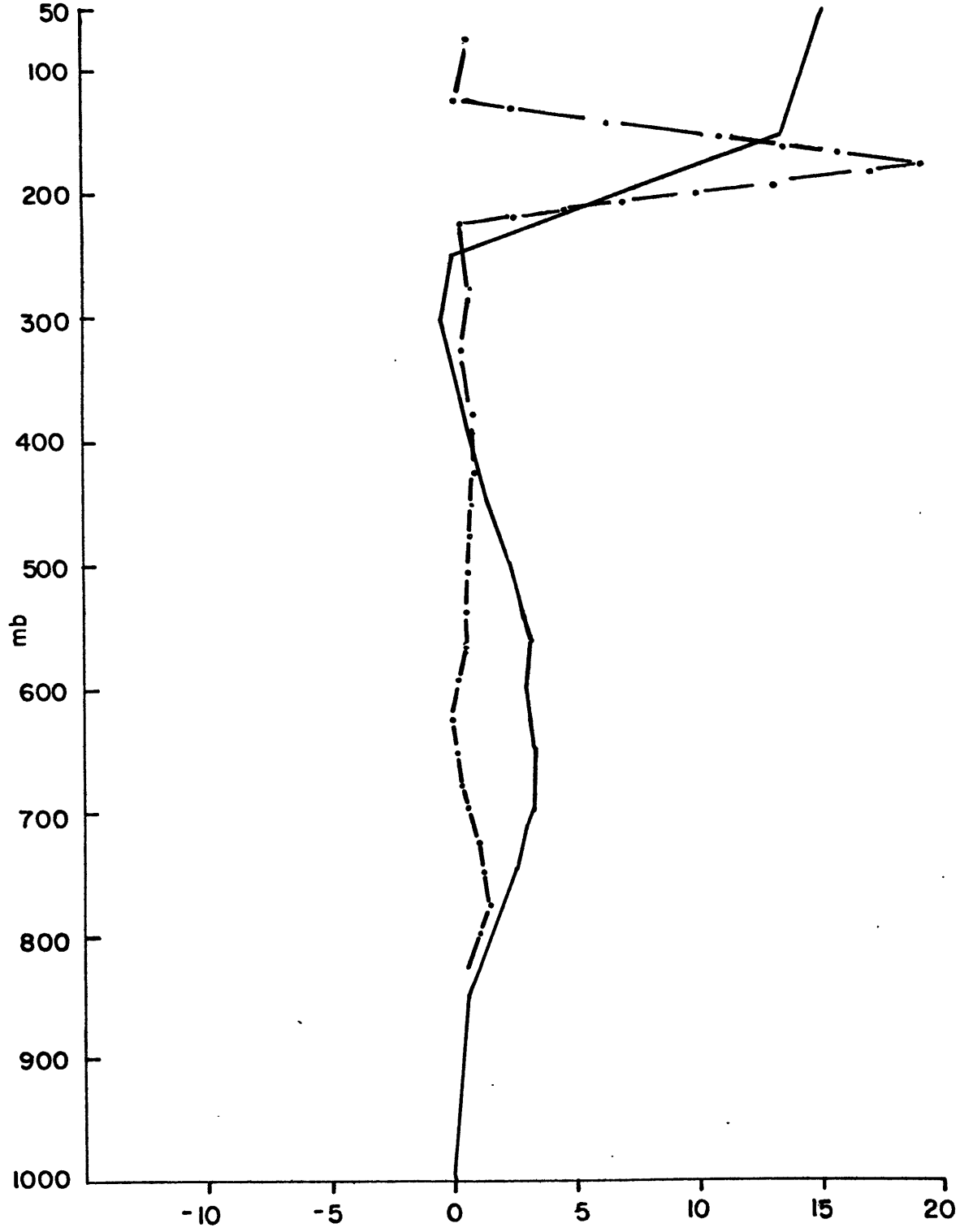

Figure 14. Distributions of vertical velocities (10^{-3} mb/s), calculated from the continuity equation (——) and the adiabatic thermodynamic equation (—·—·) for triangle CDE on August 27, 1973.

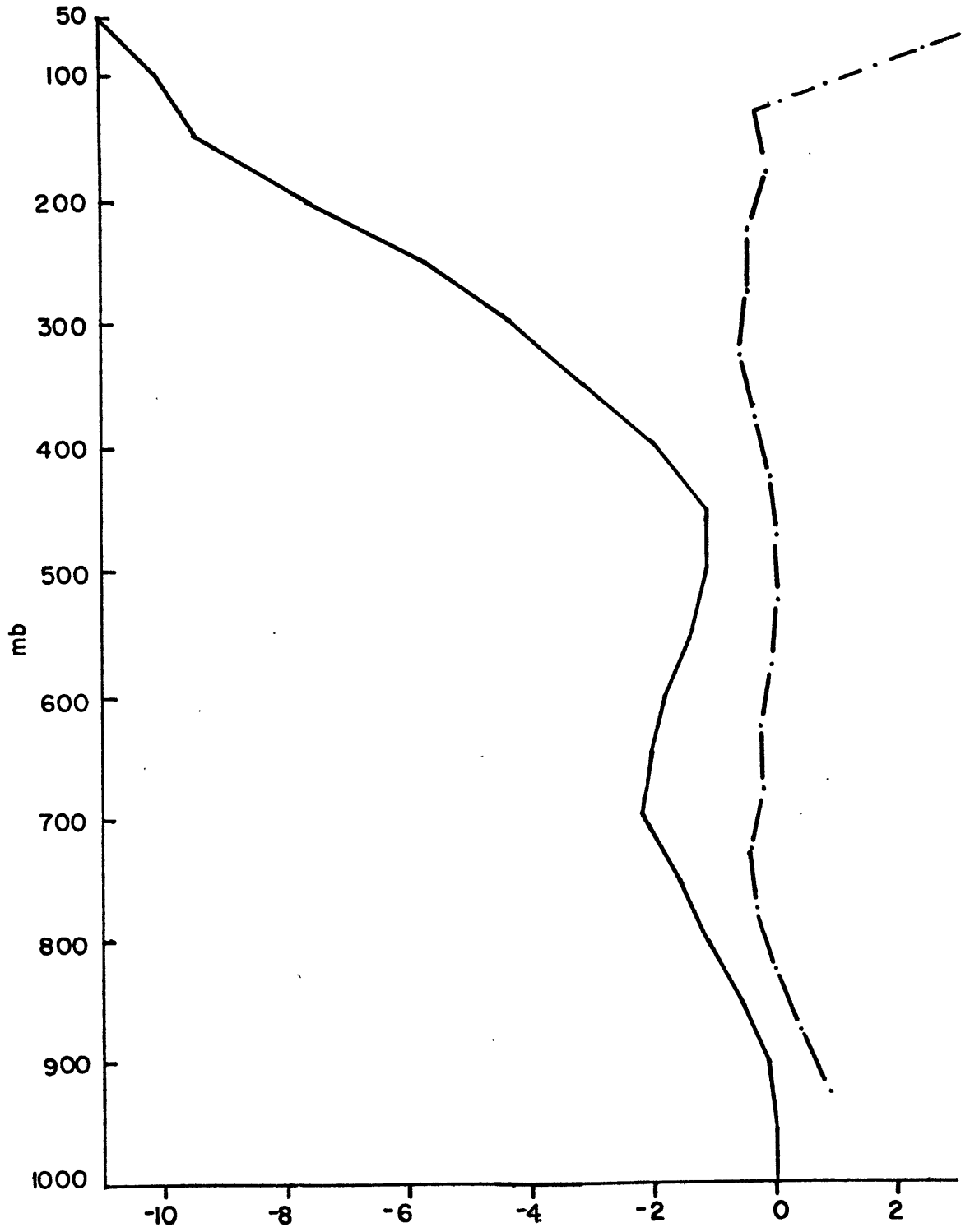

Figure 15. Distributions of vertical velocities (10^{-3} mb/s), calculated from the continuity equation (——) and the adiabatic thermodynamic equation (—·—·) for triangle DEF on August 28, 1973.

Figure 16. Distributions of vertical velocities (10^{-3} mb/s), calculated from the continuity equation (——) and the adiabatic thermodynamic equation (—·—·) for triangle EFC on August 28, 1973.

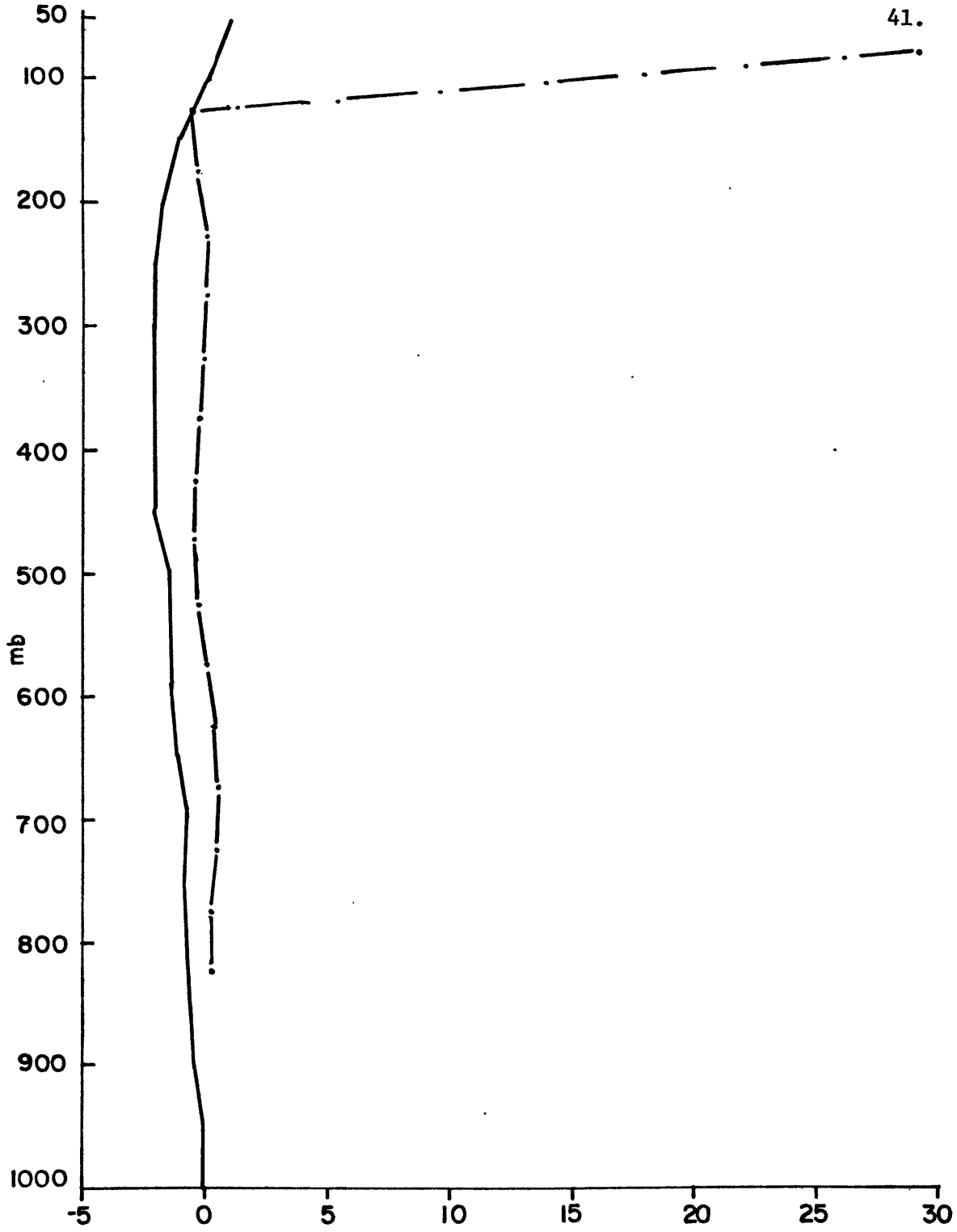

Figure 17. Distributions of vertical velocities (10^{-3} mb/s), calculated from the continuity equation (——) and the adiabatic thermodynamic equation (—·—·) for triangle CDE on August 28, 1973.

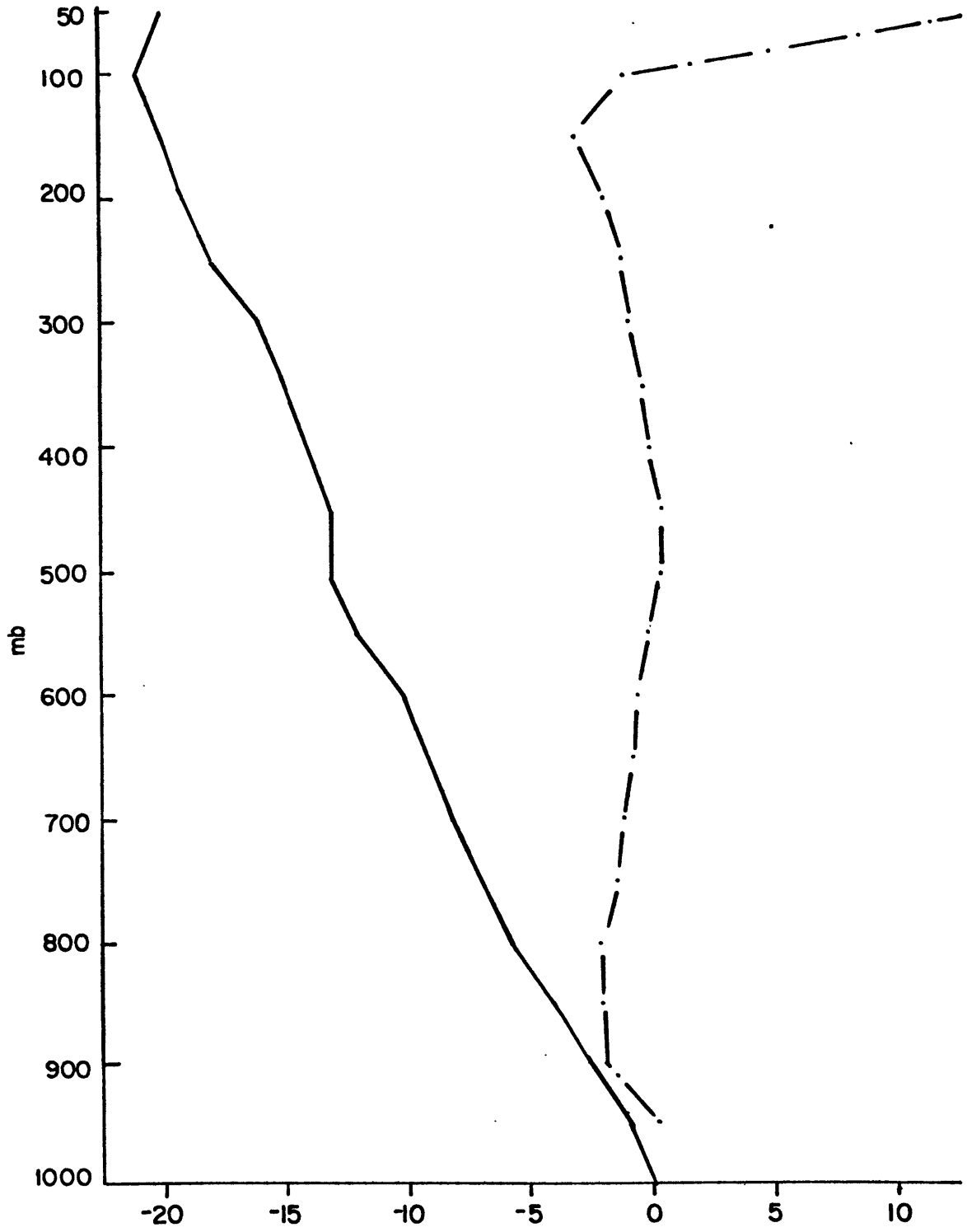

Figure 18. Distributions of vertical velocities (10^{-3} mb/s), calculated from the continuity equation (——) and the adiabatic thermodynamic equation (—·—·) for triangle ACE on August 28, 1973.

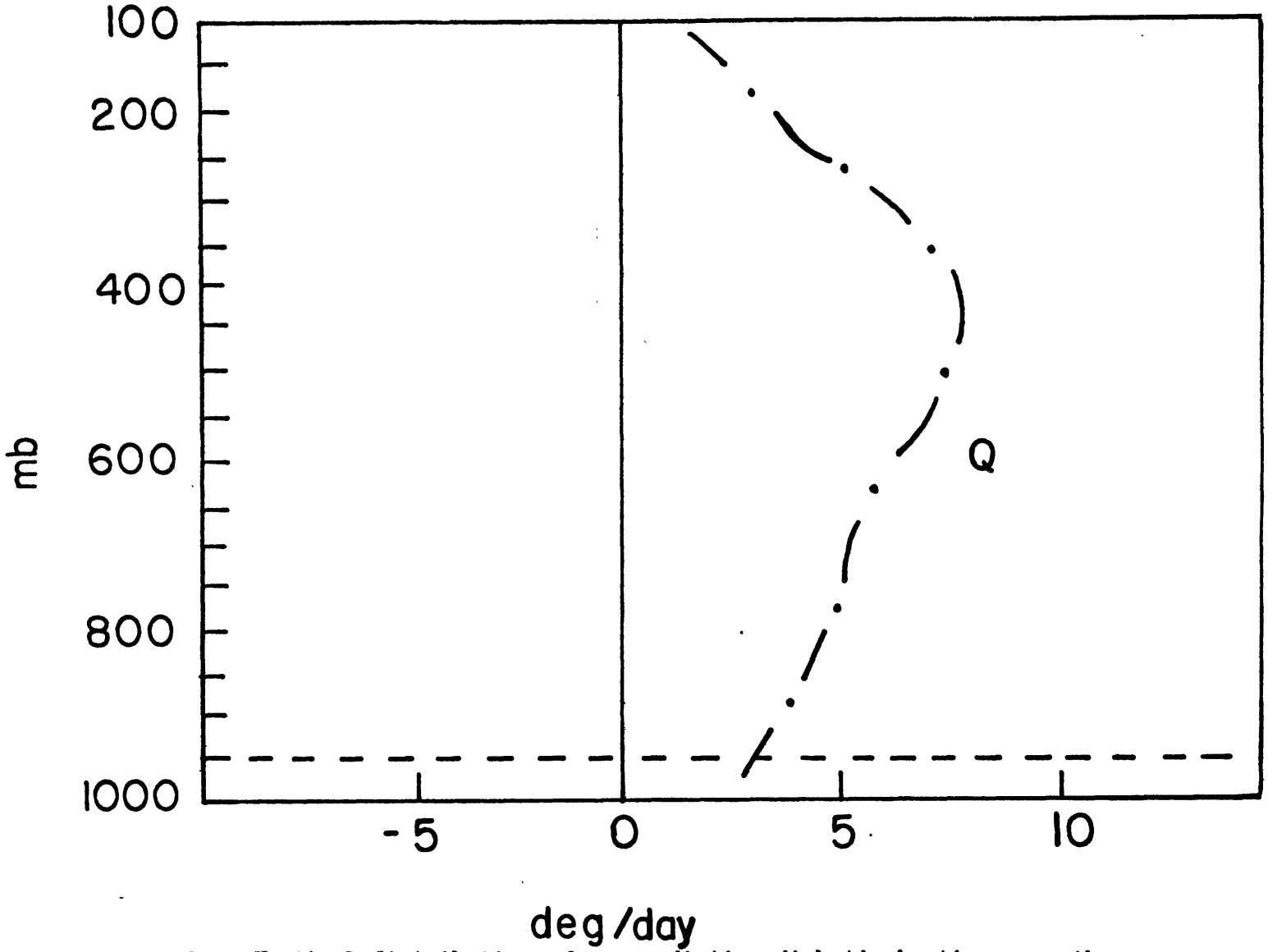

Figure 19. Vertical distribution of non-radiative diabatic heating over the Marshall Islands region (From: Yanai, et. al., 1973)

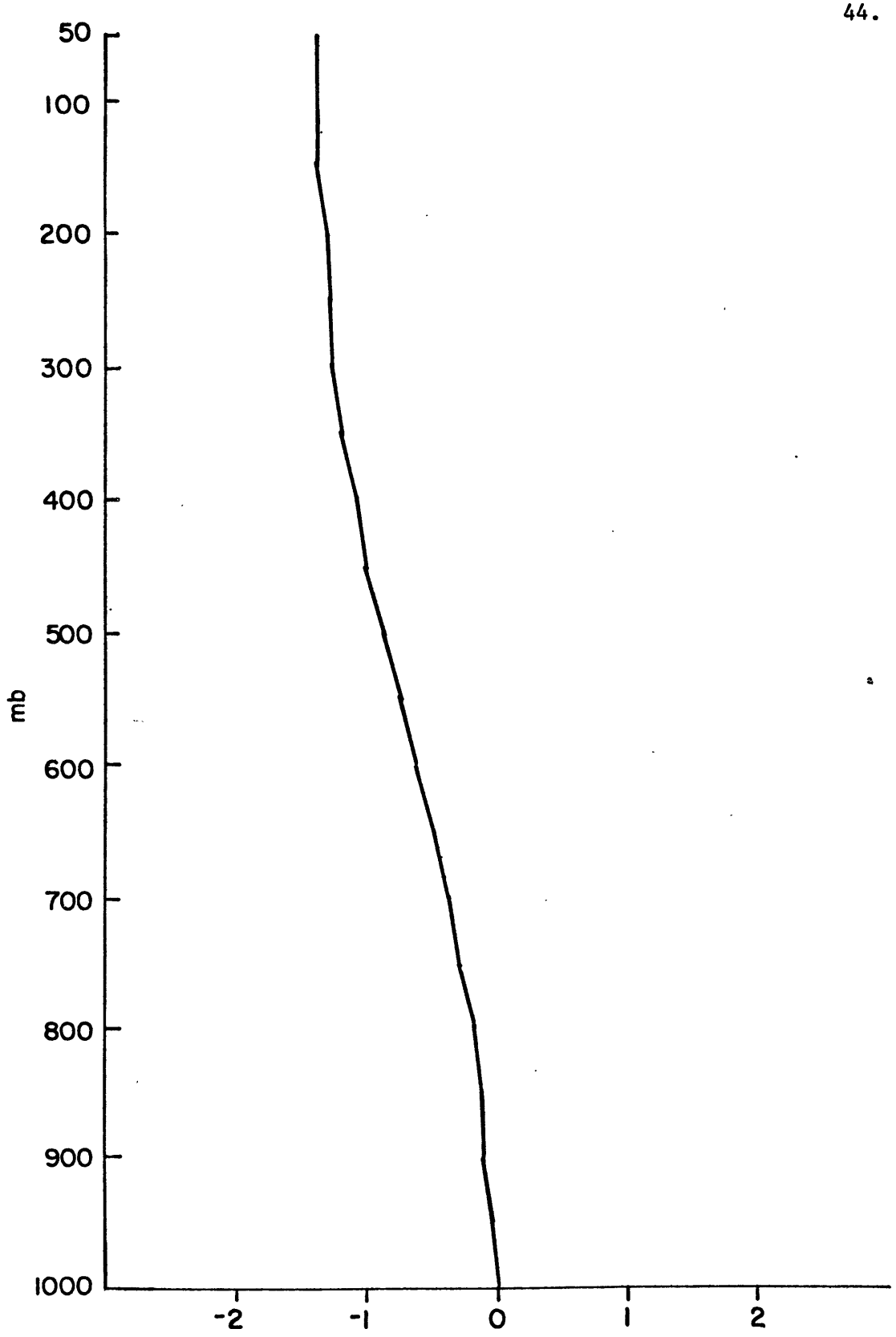

Figure 20. Distribution of vertical velocities (10^{-2} mb/s), calculated from the continuity equation for triangle HIJ on August 26, 1973.

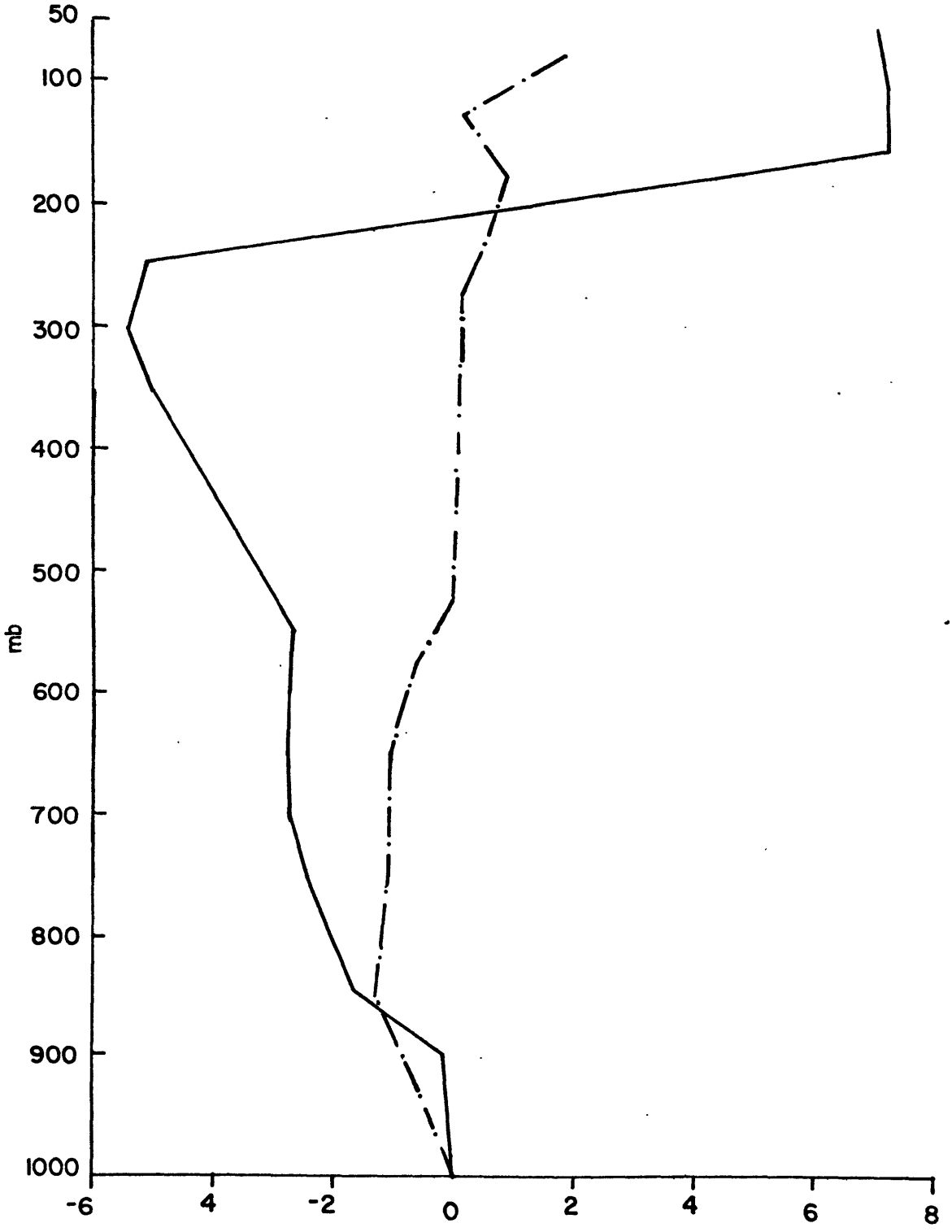

Figure 21. Distributions of vertical velocities (10^{-3} mb/s) calculated from the continuity equation (——) and the adiabatic thermodynamic equation (—·—·) for triangle HIJ on August 27, 1973.

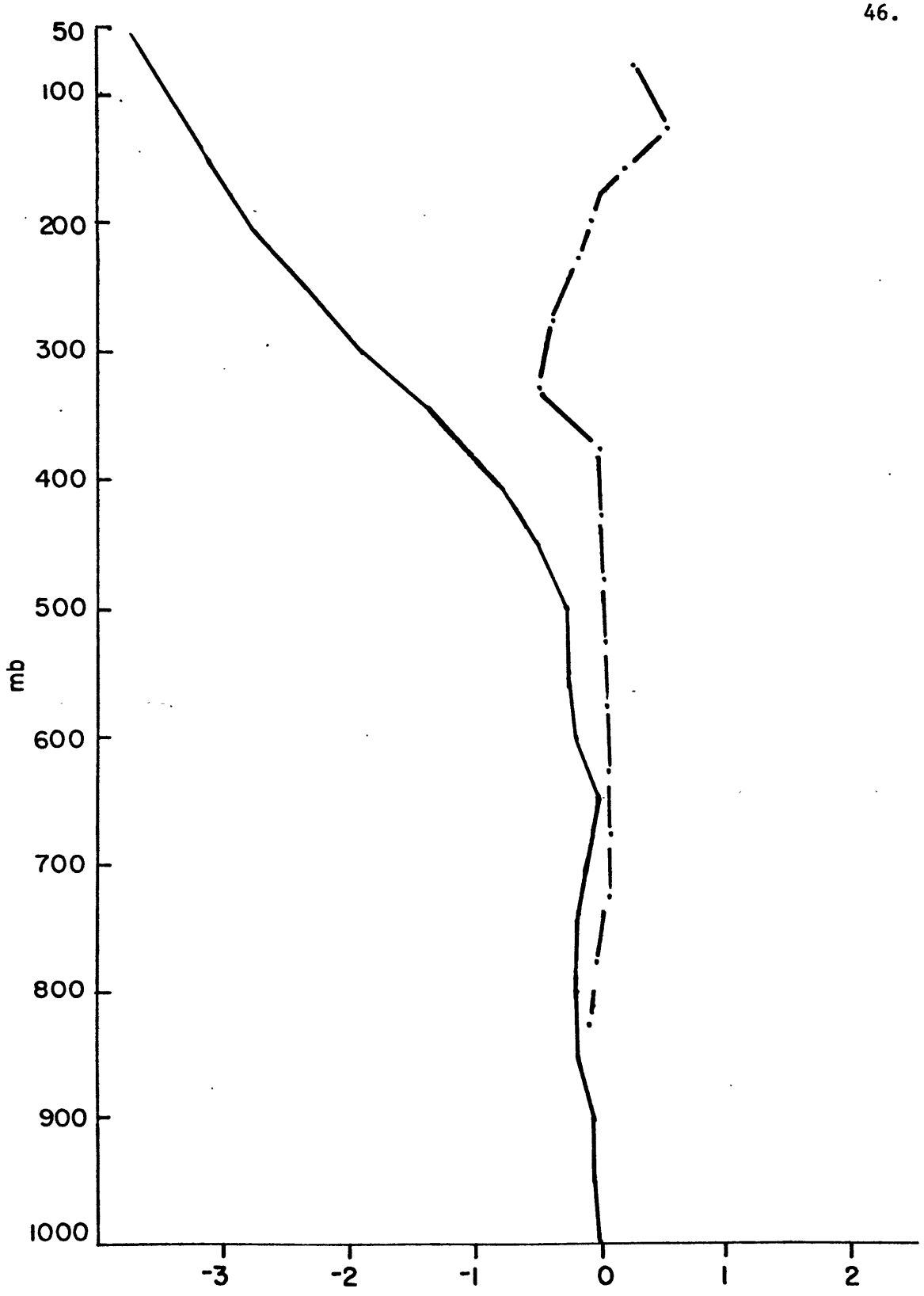

Figure 22. Distributions of vertical velocities (10^{-3} mb/s) calculated from the continuity equation (——) and the adiabatic thermodynamic equation (—·—·) for triangle HIJ on August 28, 1973.

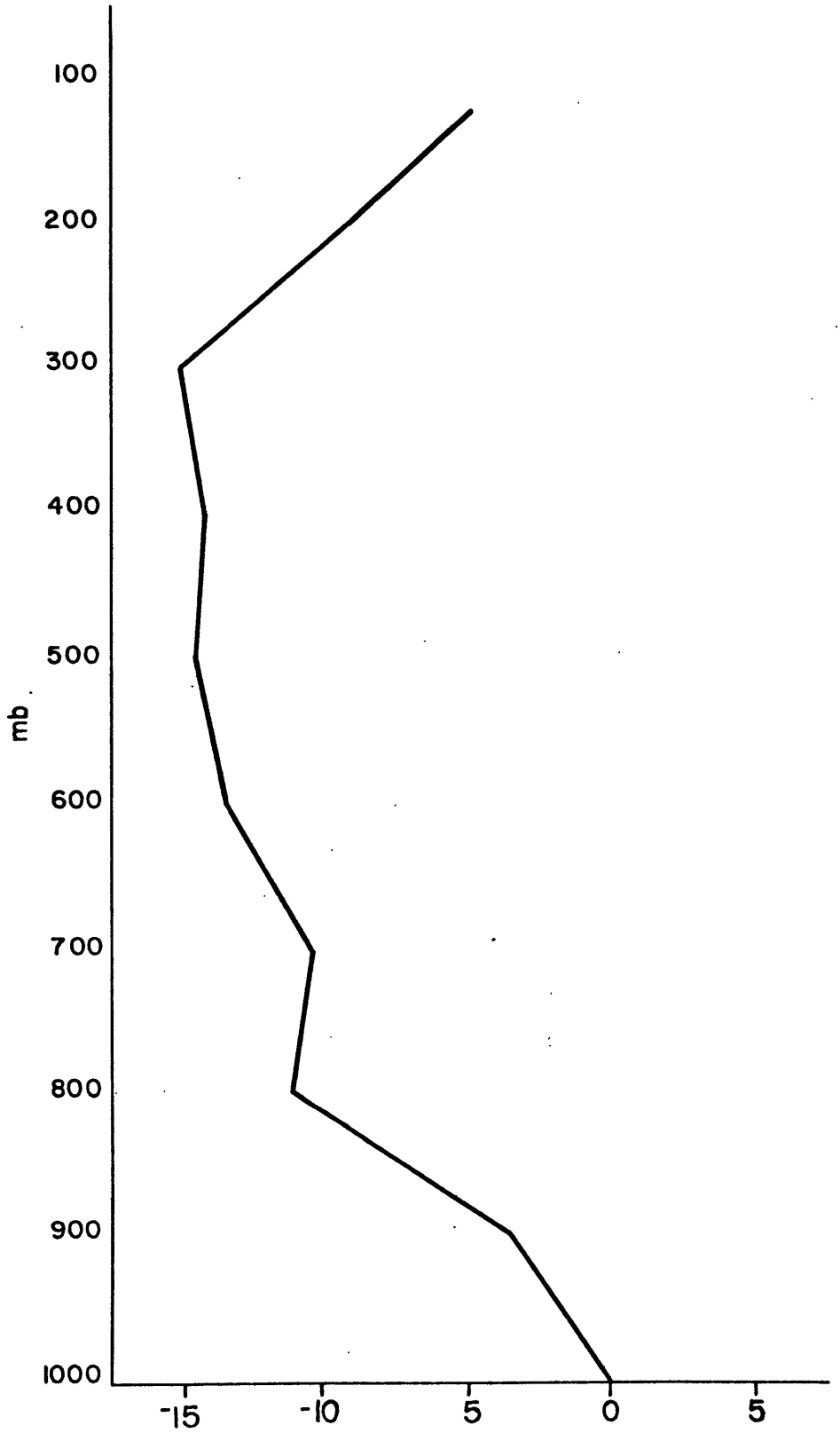

Figure 23. Distribution of vertical velocities (10^{-3} mbs^{-1}), calculated from the diabatic thermodynamic equation, Eqn. 3.4, and the Yanai profile (1973) for triangle GIJ.

and one of descending motion over northwest India and Pakistan. For example, Krishnamurti (1966), using a balance model, computed vertical velocities in the monsoon field between latitudes 6°N and 48°N and longitudes 30°E and 108°E. He found general rising motion in the northeastern parts of the monsoon trough with maximum intensity of 1 cms^{-1} and sinking motion to the southwest of the trough. He further remarked that there were considerable variations in the three days he studied in the form of local intense centers of rising and sinking motion.

Recently Krishnamurti (1976) studied the dynamic and synoptic aspects of a monsoon disturbance. Diagnostic vertical motions were evaluated using the three-dimensional omega equation and the kinematic method. He obtained maximum vertical velocities with magnitudes of 2.5×10^{-3} mbs^{-1}. His boundary conditions were $\omega = 0$ at 1000 mb and 100 mb.

A comparison of his two methods for the three days were: i) the kinematic vertical velocity values are two to three times larger than vertical velocity values from the omega equation; ii) the level of non-divergence is slightly higher for the kinematic vertical velocities, however, both were close to the 700 mb level for the first day; iii) there is a region of more pronounced subsidence over the Arabian Sea and east of the depression. Both methods agree in the position of the maximum upward vertical velocity and the location of the vertical motion centers agree well with the observed regions of rainfall in the monsoon depression.

Rao and Rajamani (1972) have also computed vertical motions for a monsoon depression. They noted a level of non-divergence at 700 mb

and rising motion centers to the west of the storm center.

The magnitudes of the velocities we obtained from the kinematic method agree with results obtained by Krishnamurti (1976) except that maximum ω's are obtained around the 500 mb level in our study and at the 700 mb level in Krishnamurti (1976). The velocities computed within the heavy precipitation areas also agree with results obtained by Rao and Rajamani (1972). Thus we feel confident in the plausibility of our results.

Figures 24-26 show horizontal cross-sections of the vertical velocities computed from Equation 3.6 at the centroids for the small triangles around 24°N latitude. From these figures we can see upward and compensating downward motion across the latitude belt. This is not an uncommon phenomenon. Observations indicate that most precipitation in tropical systems is of convective origin and is concentrated in a comparatively small number of deep vigorous cumulus convection cells. These cells occupy only a small percentage of the area of the tropics in active disturbances. Thus, upward motion can be predominant in one triangle while subsidence predominates in the adjacent triangle.

Figures 27-28 show the cross-section of vertical velocities computed from Equation 3.3. As can be seen, velocities computed from Equations 3.3 and 3.6 indicate the same positions of upward and downward motion. However, as mentioned earlier, the vertical velocities calculated from Equation 3.3 are an order of magnitude smaller than the velocites computed by Equation 3.6.

Figures 29-31 represent a vertical cross-section of vertical velocities computed from Equation 3.6 for the larger triangles around 81°E

longitude. From Figure 29 we can see there is net upward motion on the 26th of August. As the trough propagates westward, the magnitude of the vertical velocities decreases. When the trough has moved completely inland (August 28th) compensating downward motion east of the trough begins in the Northern Indian latitudes (Figure 31).

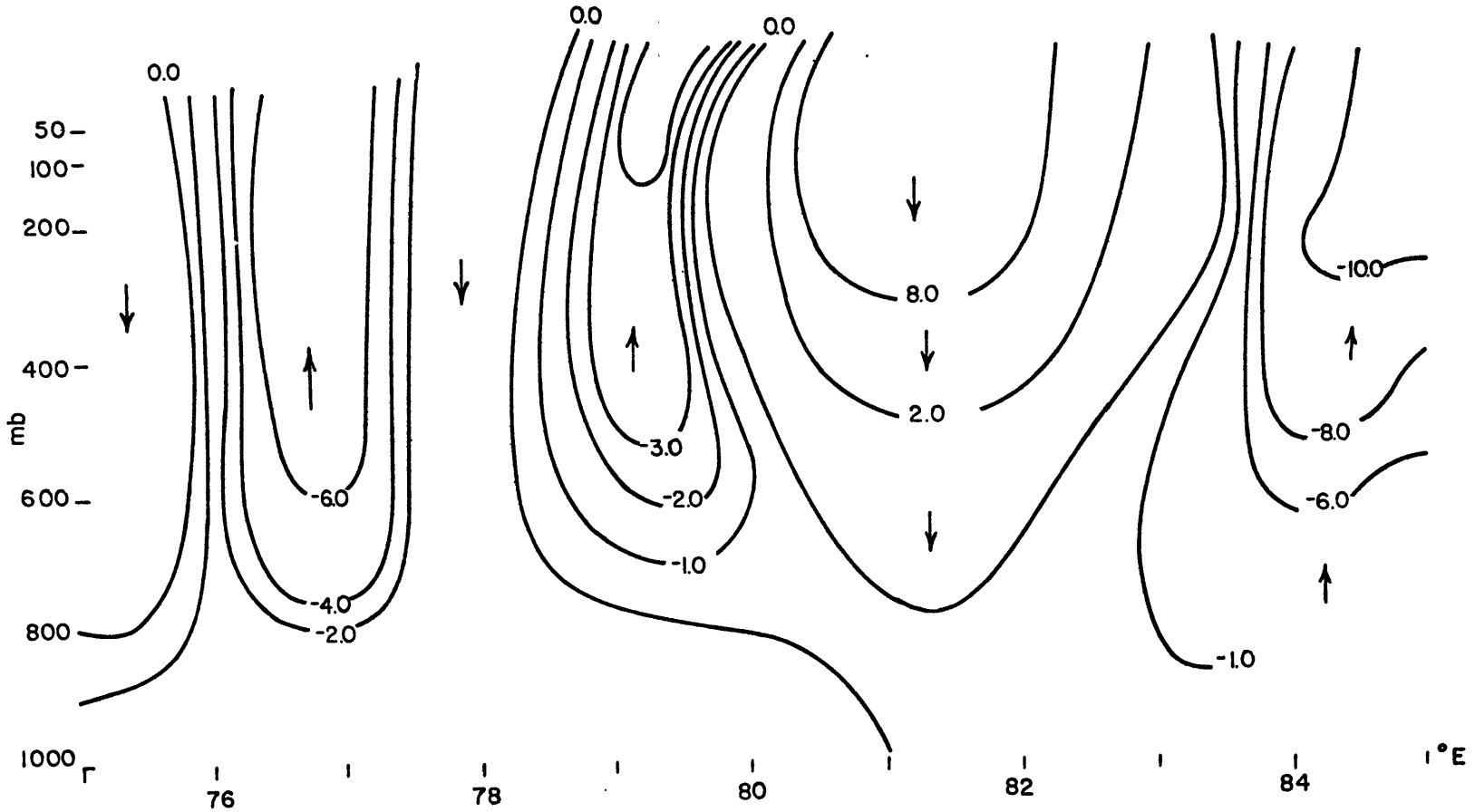

Figure 24. Horizontal cross-section of the vertical velocities (10^{-3} mb/s) calculated from the continuity equation around 24°N latitude and between 73°-85°E longitude on August 26, 1973.

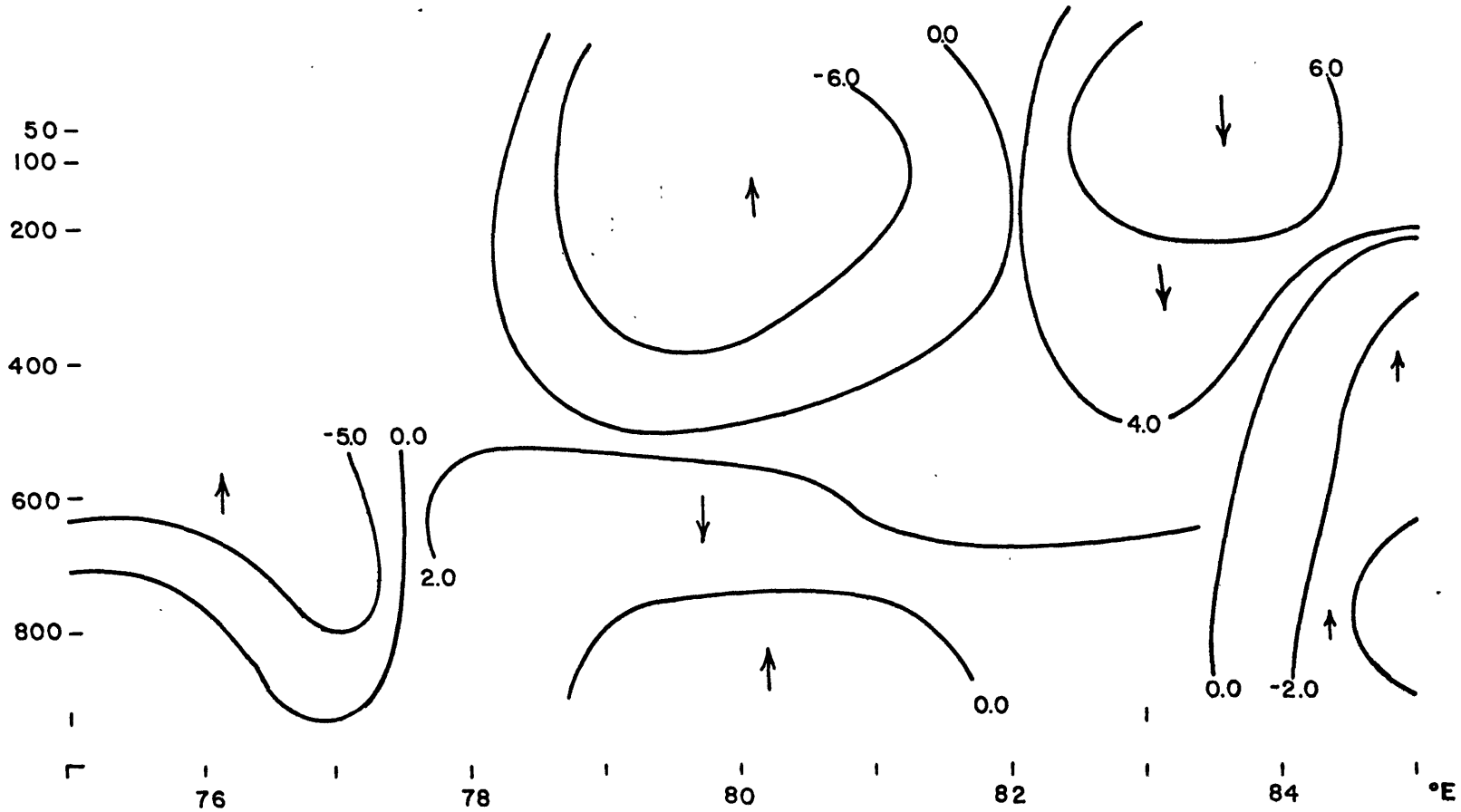

Figure 25. Horizontal cross-section of the vertical velocities (10^{-3} mb/s) calculated from the continuity equation around 24°N latitude and between 73°-85°E longitude on August 27, 1973.

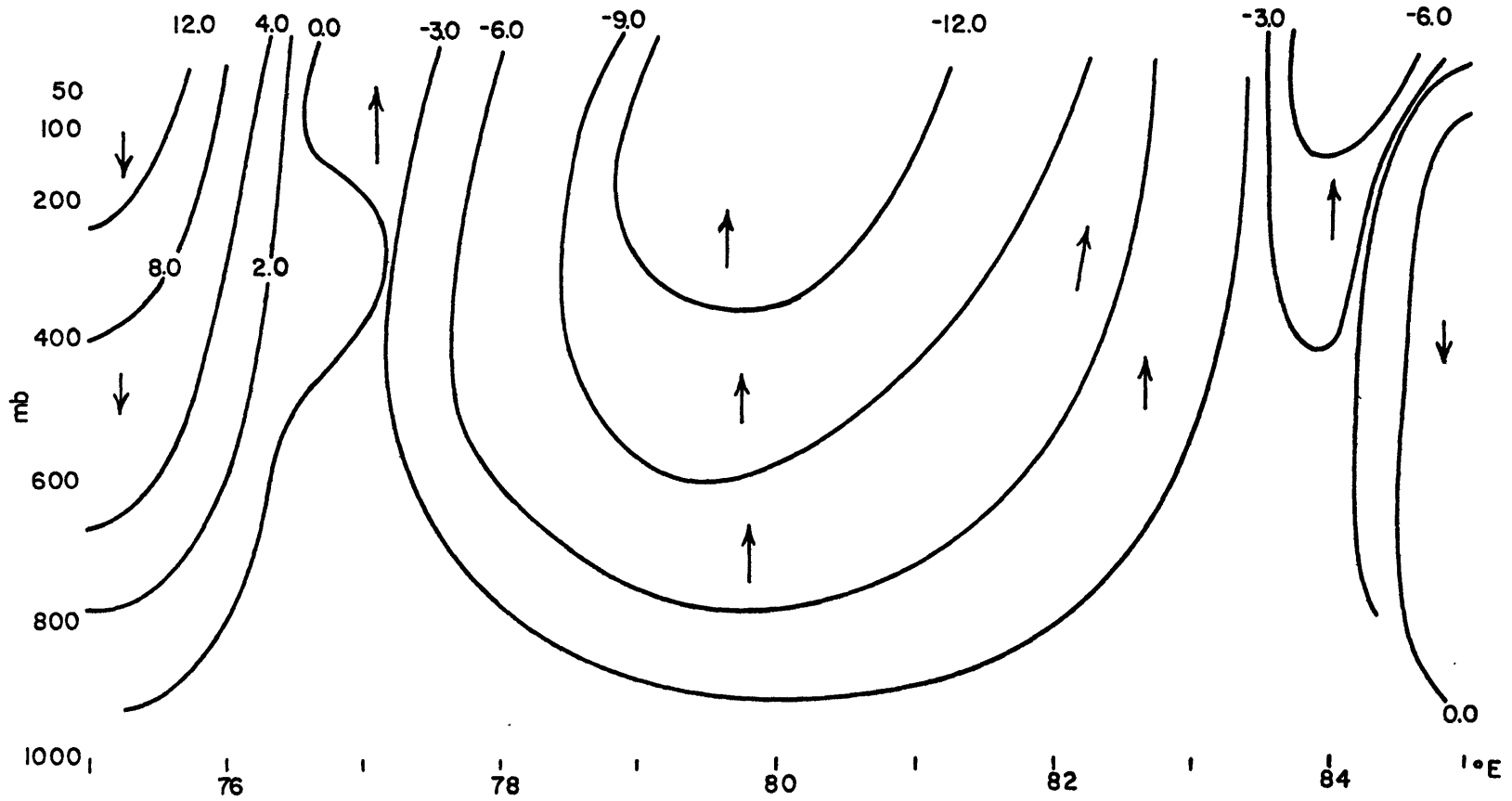

Figure 26. Horizontal cross-section of the vertical velocities (10^{-3} mb/s) calculated from the continuity equation around 24°N latitude and between 73°-85°E longitude on August 28, 1973.

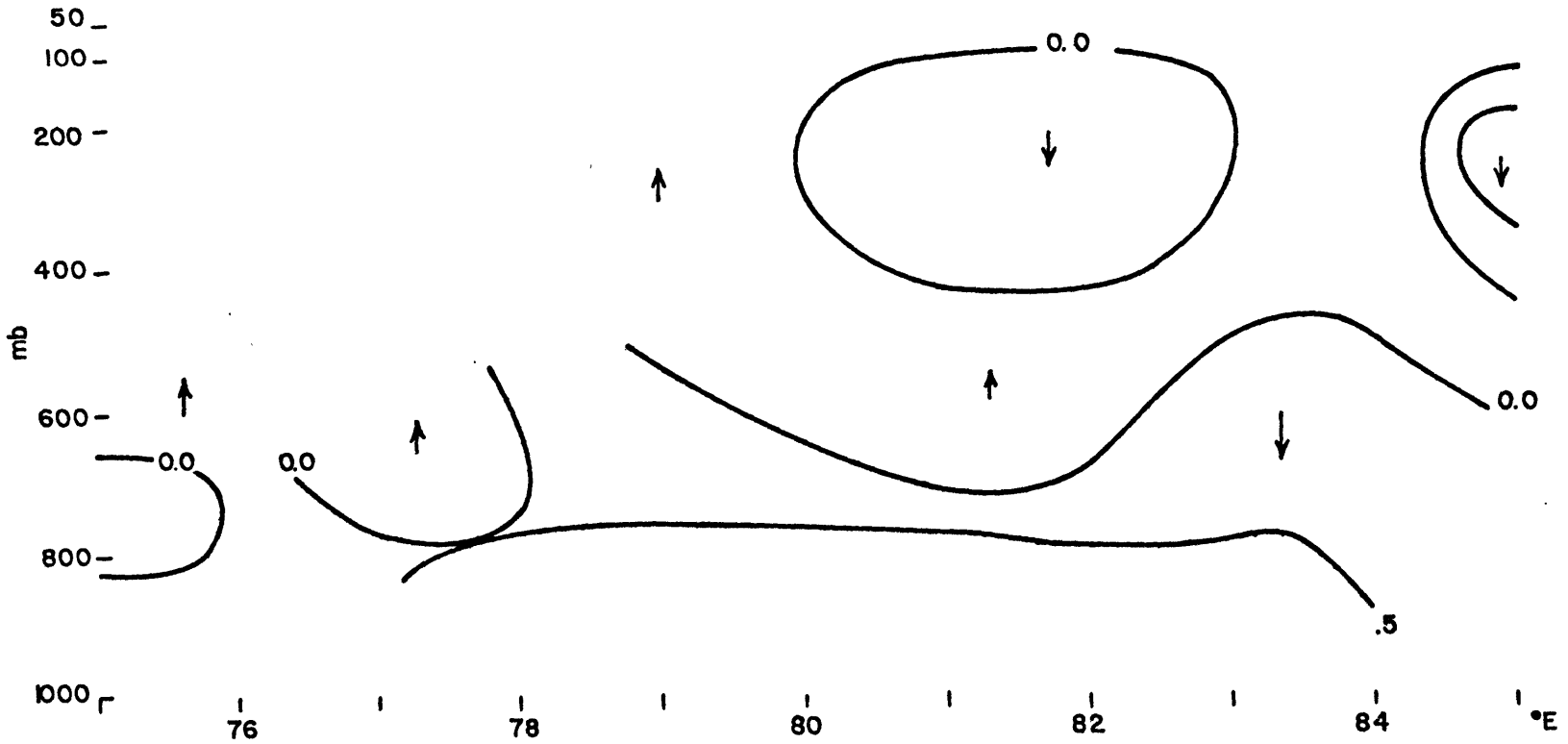

Figure 27. Horizontal cross-section of the vertical velocities (10^{-3} mb/s) calculated from the adiabatic thermodynamic equation around 24°N latitude and between 73°-85°E longitude on August 27, 1973.

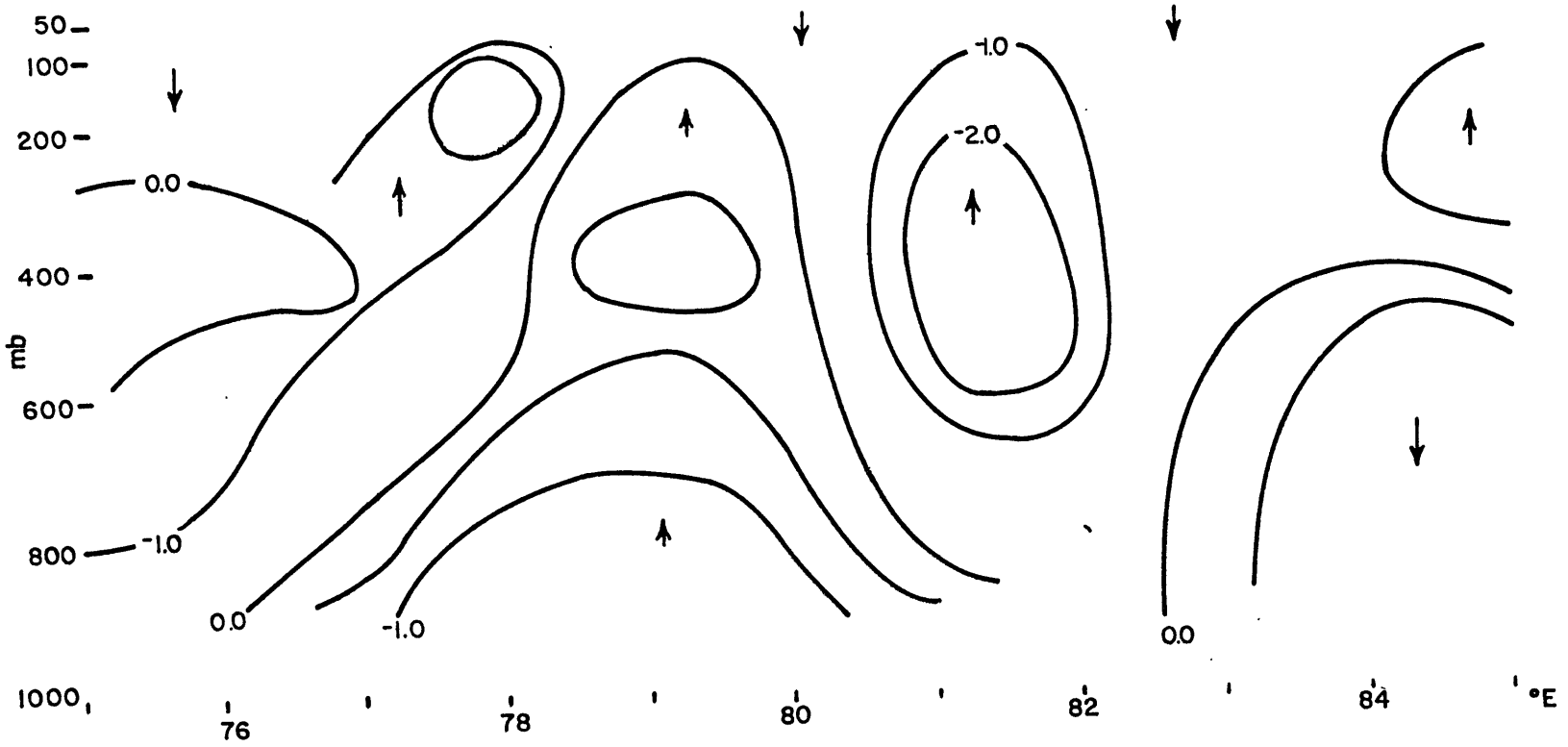

Figure 28. Horizontal cross-section of the vertical velocities (10^{-3} mb/s) calculated from the adiabatic thermodynamic equation around 24°N latitude and between 73°-85°E longitude on August 28, 1973.

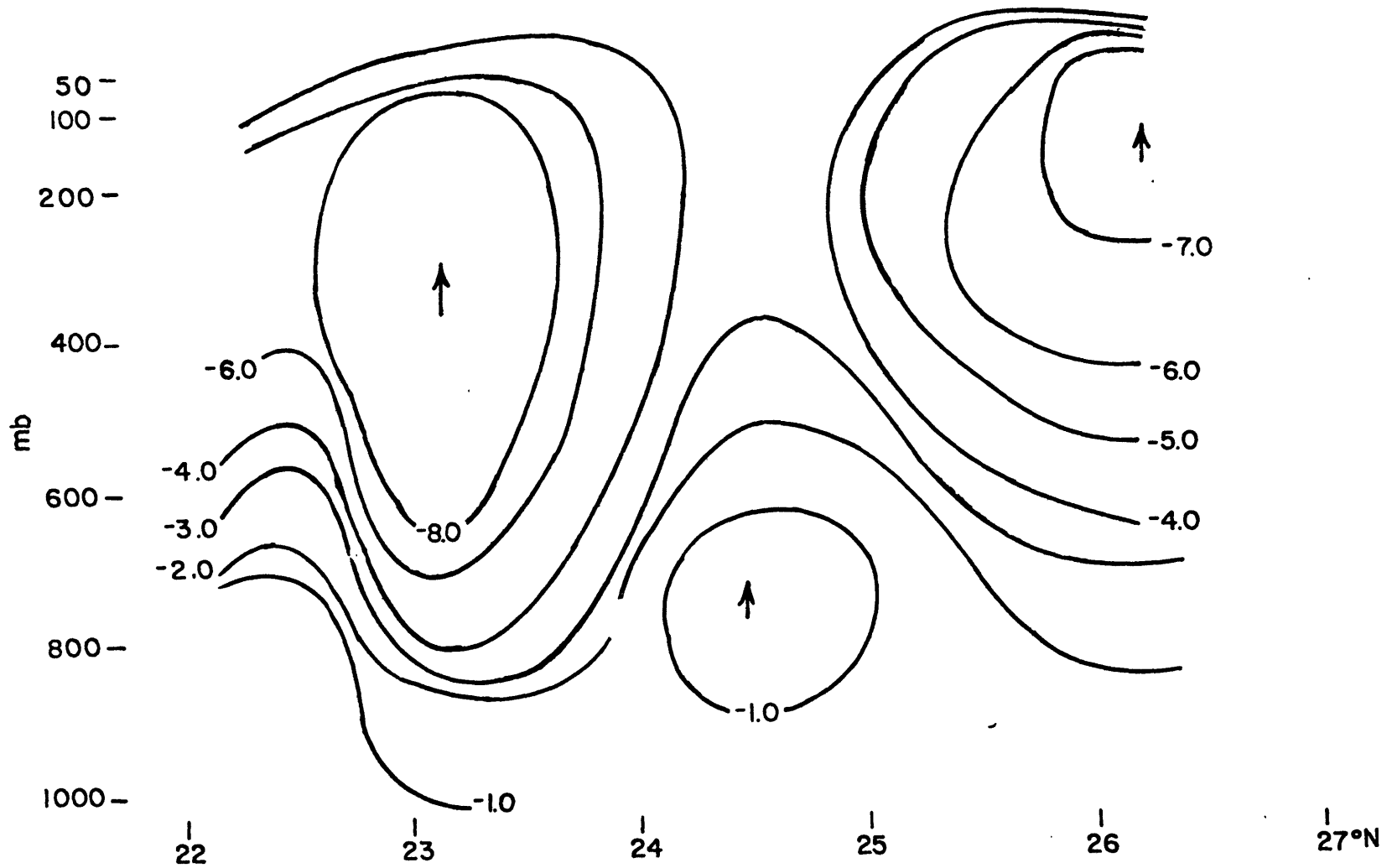

Figure 29. Vertical cross-section of vertical velocities (10^{-3} mb/s) calculated from the continuity equation between 22°-26°N latitude and around 81°E longitude on August 26, 1973.

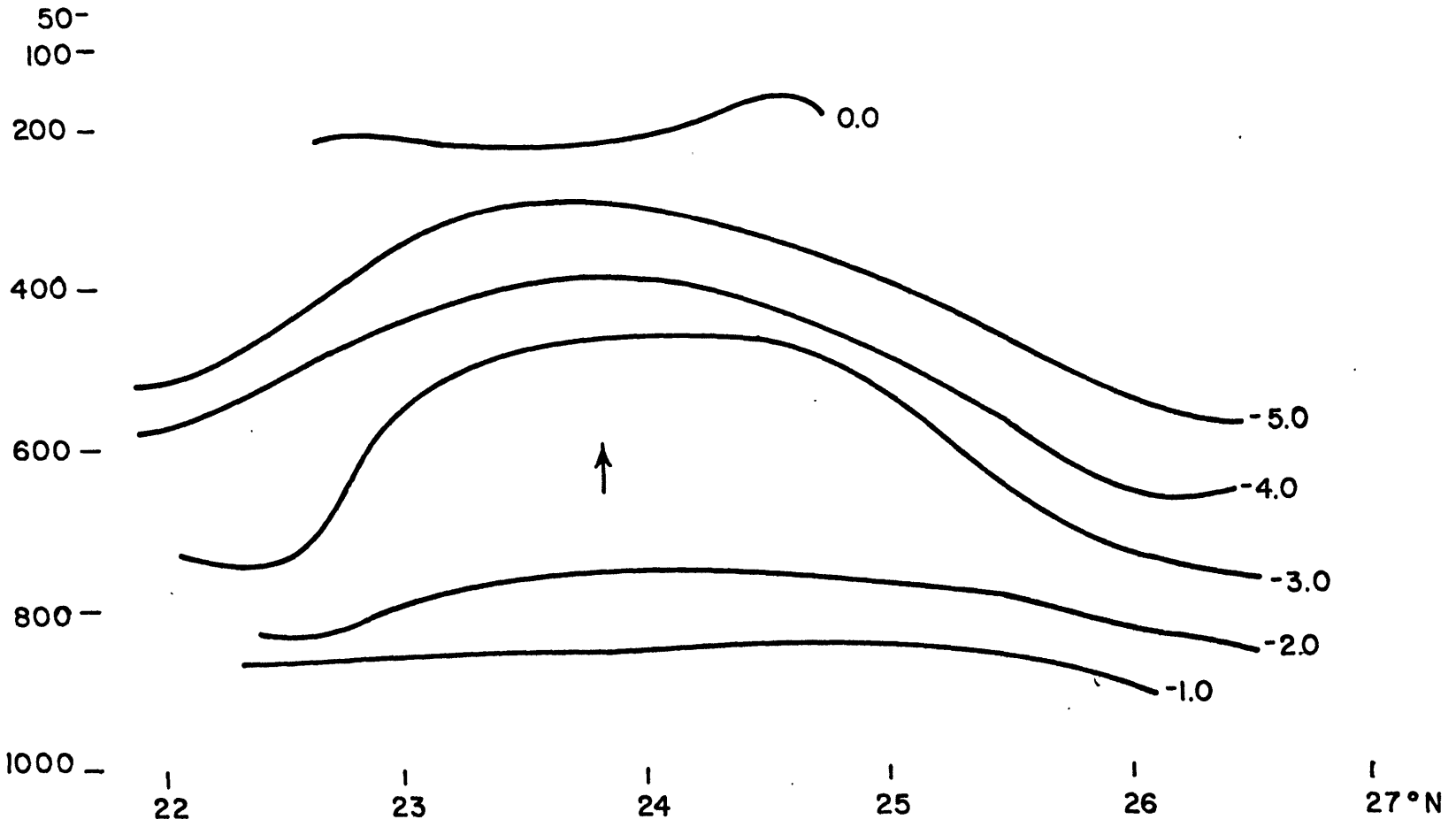

Figure 30. Vertical cross-section of vertical velocities (10^{-3} mb/s) calculated from the continuity equation between 22°-26°N latitude and around 81°E longitude on August 27, 1973.

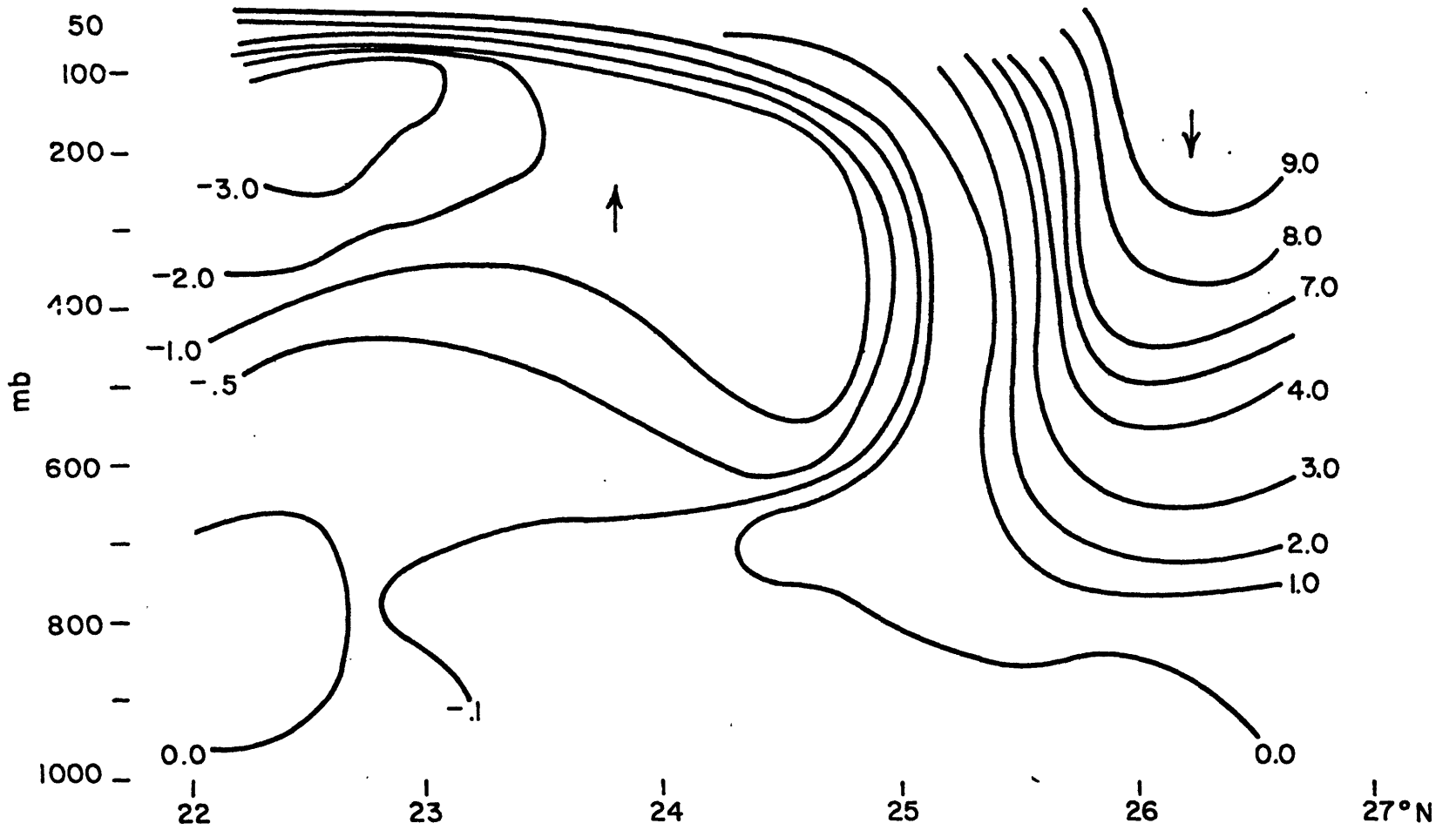

Figure 31. Vertical cross-section of vertical velocities (10^{-3} mb/s) calculated from the continuity equation between 22°-26°N latitude and around 81°E longitude on August 28, 1973.

CHAPTER 4

Absolute Vorticity and Rainfall Correlations

In this chapter the distribution of absolute vorticity and rainfall in the monsoon region are checked for consistency with the computed vertical velocities.

The vorticity equation may be written as

$$\frac{1}{(\zeta + f)} \frac{d}{dt}(\zeta + f) = -\nabla_H \cdot V \qquad (4.1)$$

for synoptic scale motions where f is the Coriolis parameter and ζ the relative vorticity (Holton, 1972). Thus, the fractional change in the absolute vorticity is proportional to the horizontal convergence.

Figure 32 from Holton (1972, pg. 109) shows schematically that the relative vorticity is a maximum on the 500 mb trough line and the mid-tropospheric convergence of relative vorticity is a maximum 90° to the west. As the air returns northward on the eastern side of the trough, the relative vorticity decreases where convergence is a minimum. The vertical motions computed take place at essentially the same latitude, and there is no appreciable change in f. Thus, convergence increases the absolute vorticity and rainy areas should coincide with areas of updraft and an increase in the absolute vorticity.

Daggapaty (1972) conducted analyses of the terms in the vorticity equation using observed quantities to explain the westward passage of the monsoon. His analyses also showed that the convergence term of the vorticity equation is largest west of the depression and horizontal

advection of absolute vorticity is largest east of the depression.

Figures 33-35 show the distributions of absolute vorticity, rainfall, and vertical velocities computed from Equation 3.6 at 26° latitude and Figures 36-38 show the distributions of these same entities at 23° latitude on the 850 mb surface for the three days investigated.

It is very interesting to note the correlation of the distributions. The rainfall distributions and vertical velocities fit very well although the velocities calculated represent a single map time and the rainfall is the daily average of various surface stations along the latitude belt.

The maximum values of absolute vorticity are 9.5×10^{-5} s^{-1} at 26°N and 10.5×10^{-5} s^{-1} at 23° N on 8-27 and 8-28 respectively. These values can be compared with those computed by Krishnamurti in his study. He obtained a maximu value of 1.4×10^{-4} s^{-1} at about 22°N. Our values are in reasonable agreement with the value he obtained. On the third day of our study the precipitation rates show a marked increase and the absolute vorticity and the vertical velocities exhibit the same prominent feature.

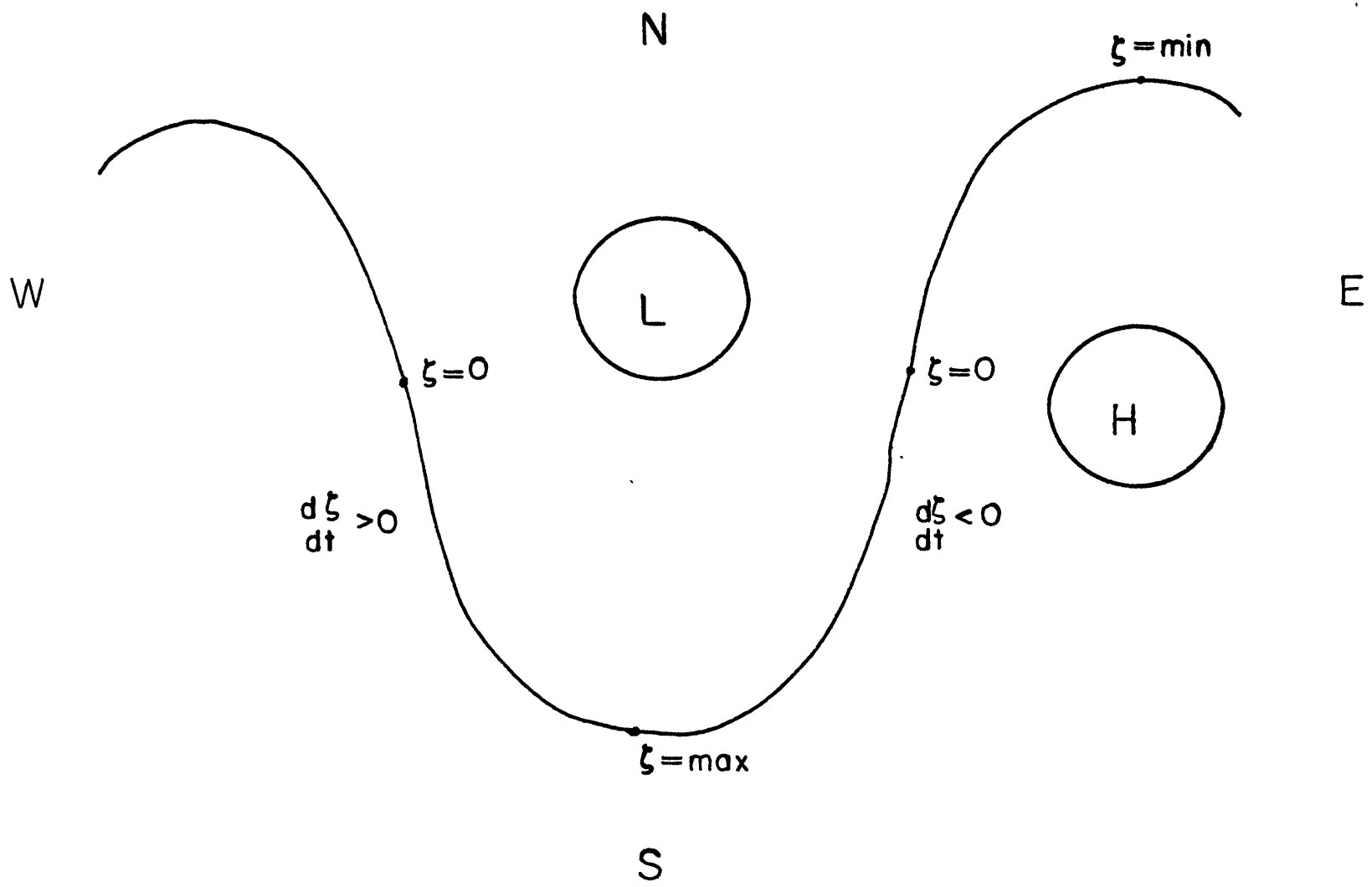

Figure 32. 500 mb geopotential field showing regions of positive and negative advection of relative vorticity.

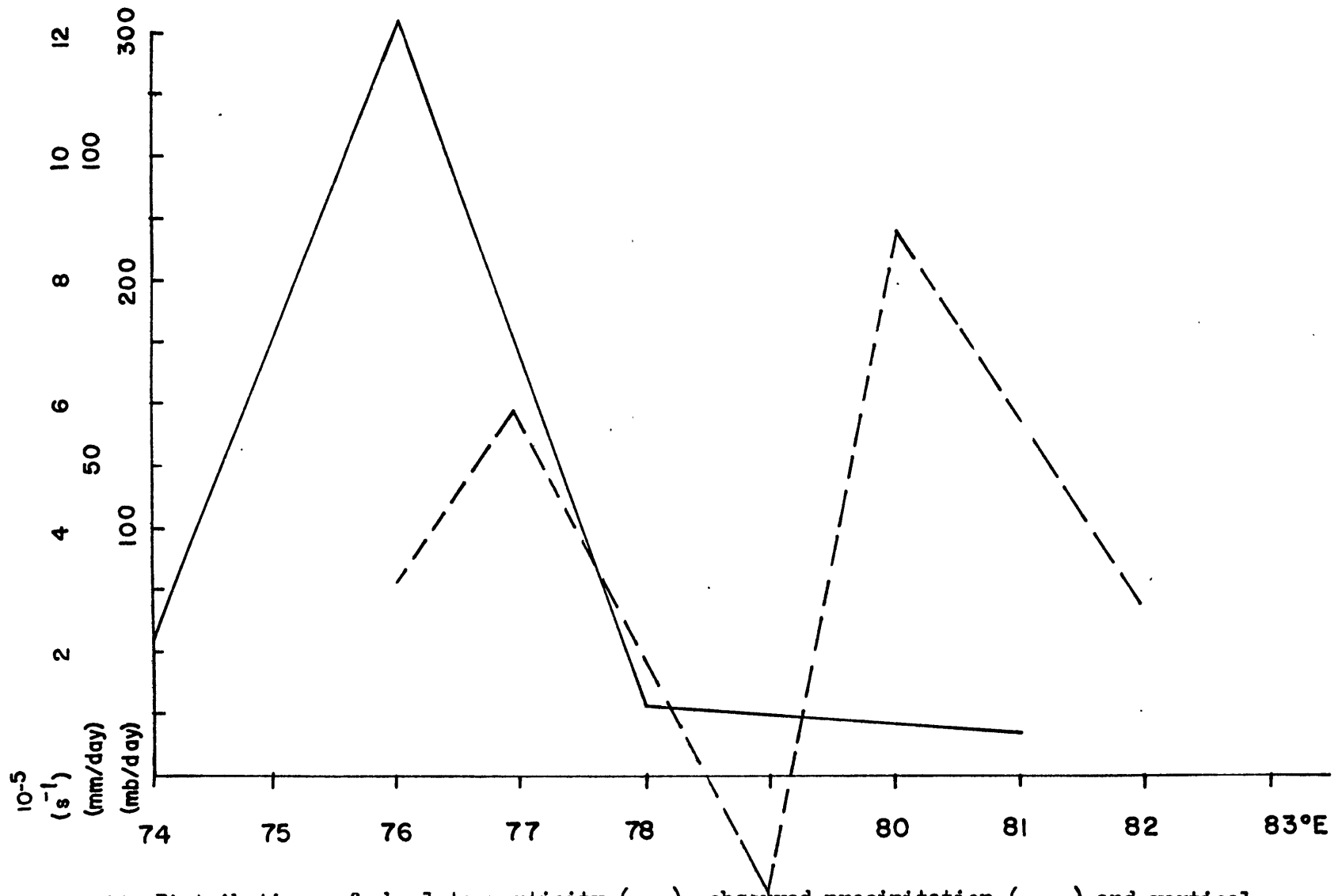

Figure 33. Distributions of absolute vorticity (-·—·-), observed precipitation (——) and vertical velocities (- - -) calculated from the continuity equation around 26°N on 8-26-73 at 850 mb.

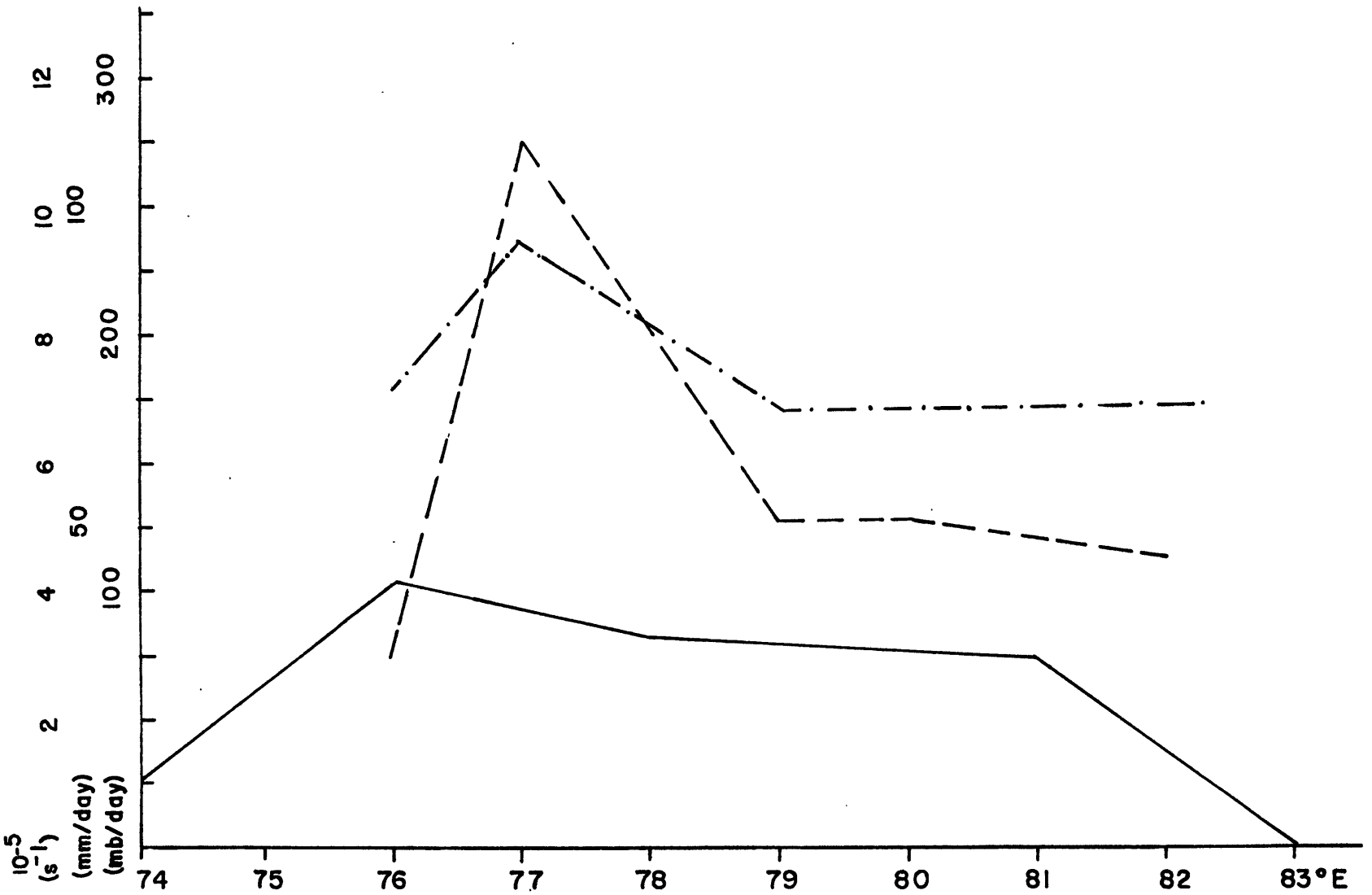

Figure 34. Distributions of absolute vorticity (—·—), observed precipitation (——) and vertical velocities (— — —) calculated from the continuity equation around 26°N on 8-27-73 at 850 mb.

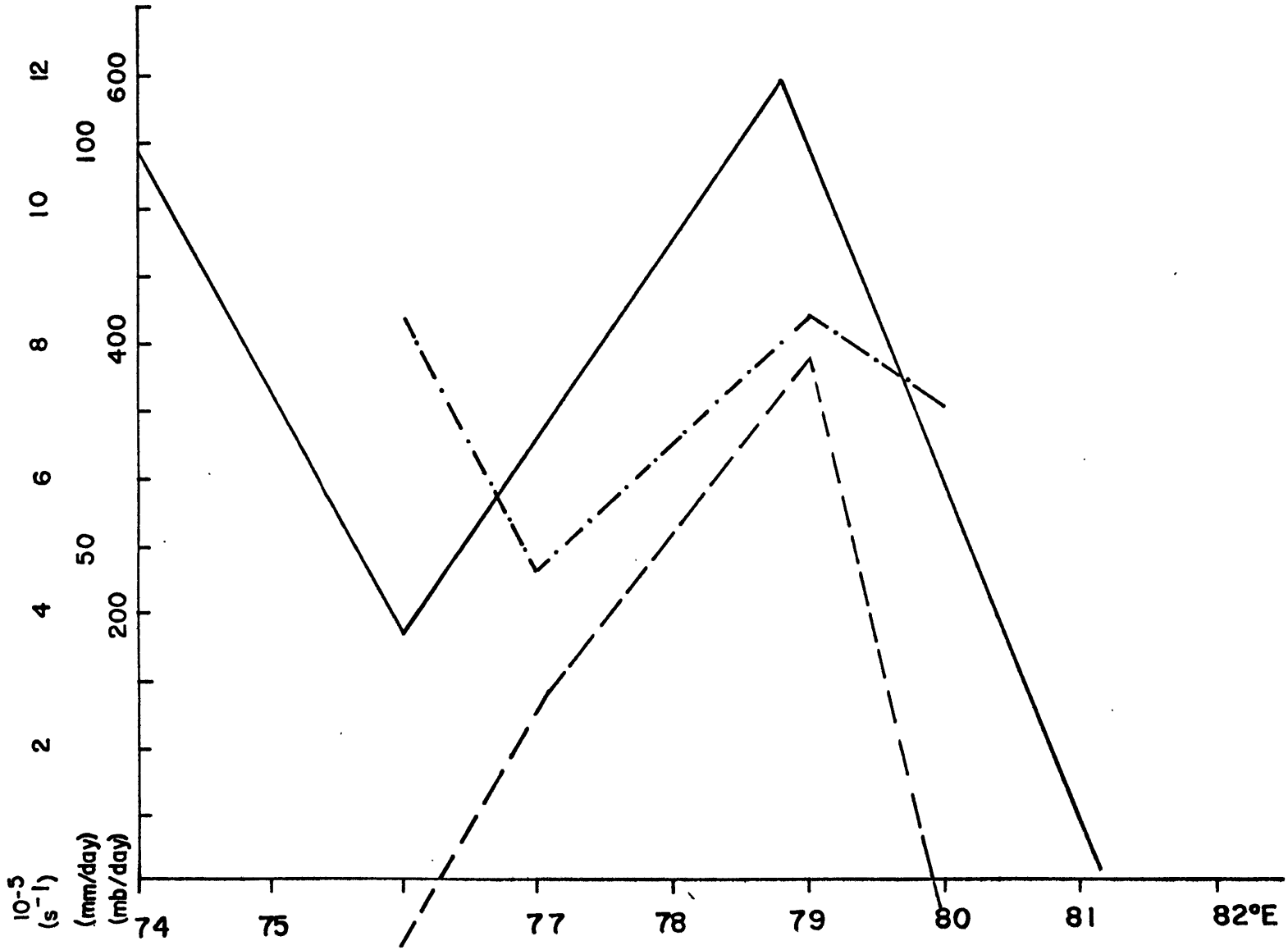

Figure 35. Distributions of absolute vorticity (—·—), observed precipitation (——) and vertical velocities (– – –) calculated from the continuity equation around 26°N on 8-28-73 at 850 mb.

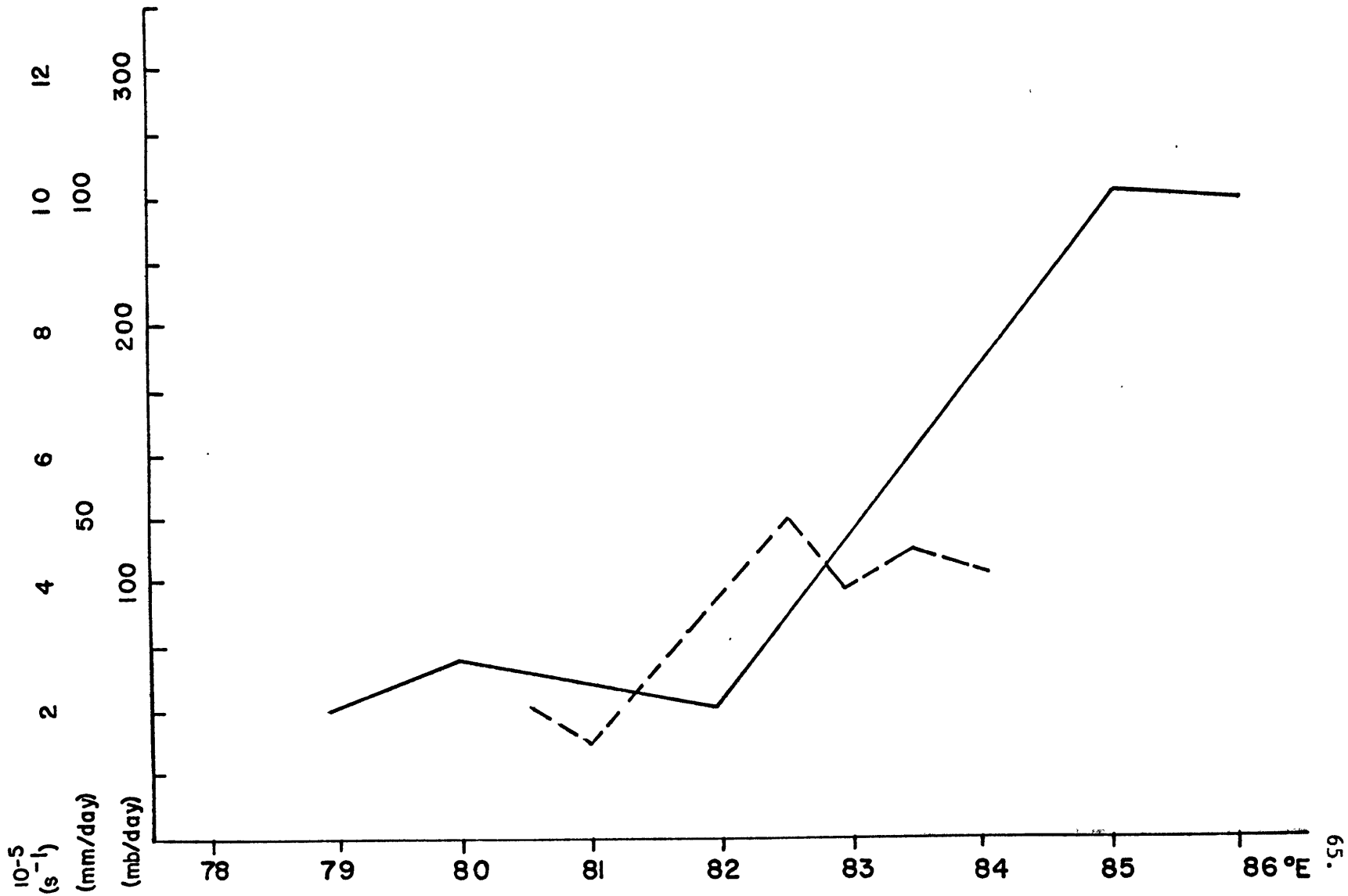

Figure 36. Distributions of absolute vorticity (—·—·), observed precipitation (——) and vertical velocities (— — —) calculated from the continuity equation around 23°N on 8-26-73 at 850 mb.

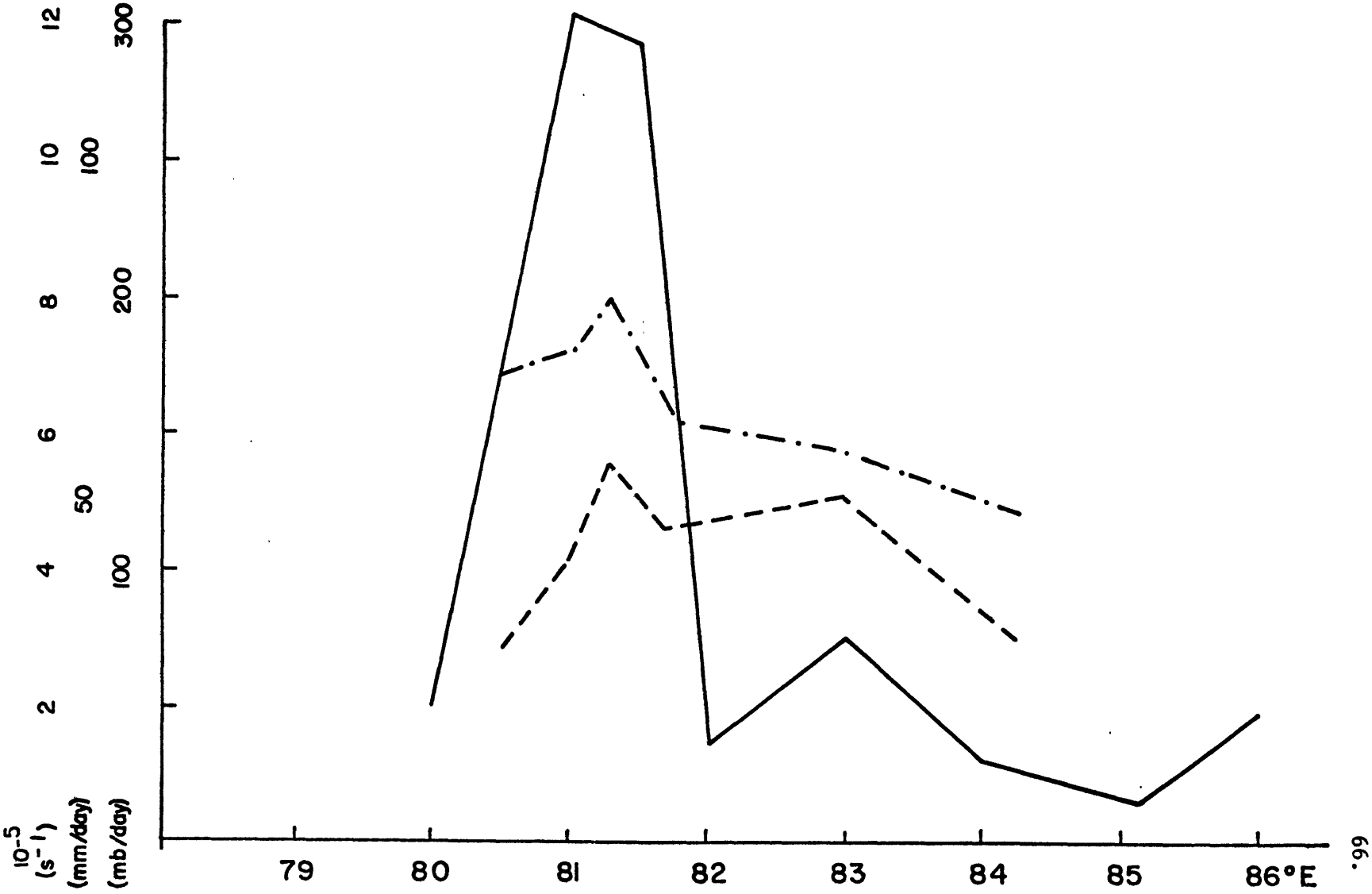

Figure 37. Distributions of absolute vorticity (-·-·-), observed precipitation (——) and vertical velocities (- - -) calculated from the continuity equation around 23°N on 8-27-73 at 850 mb.

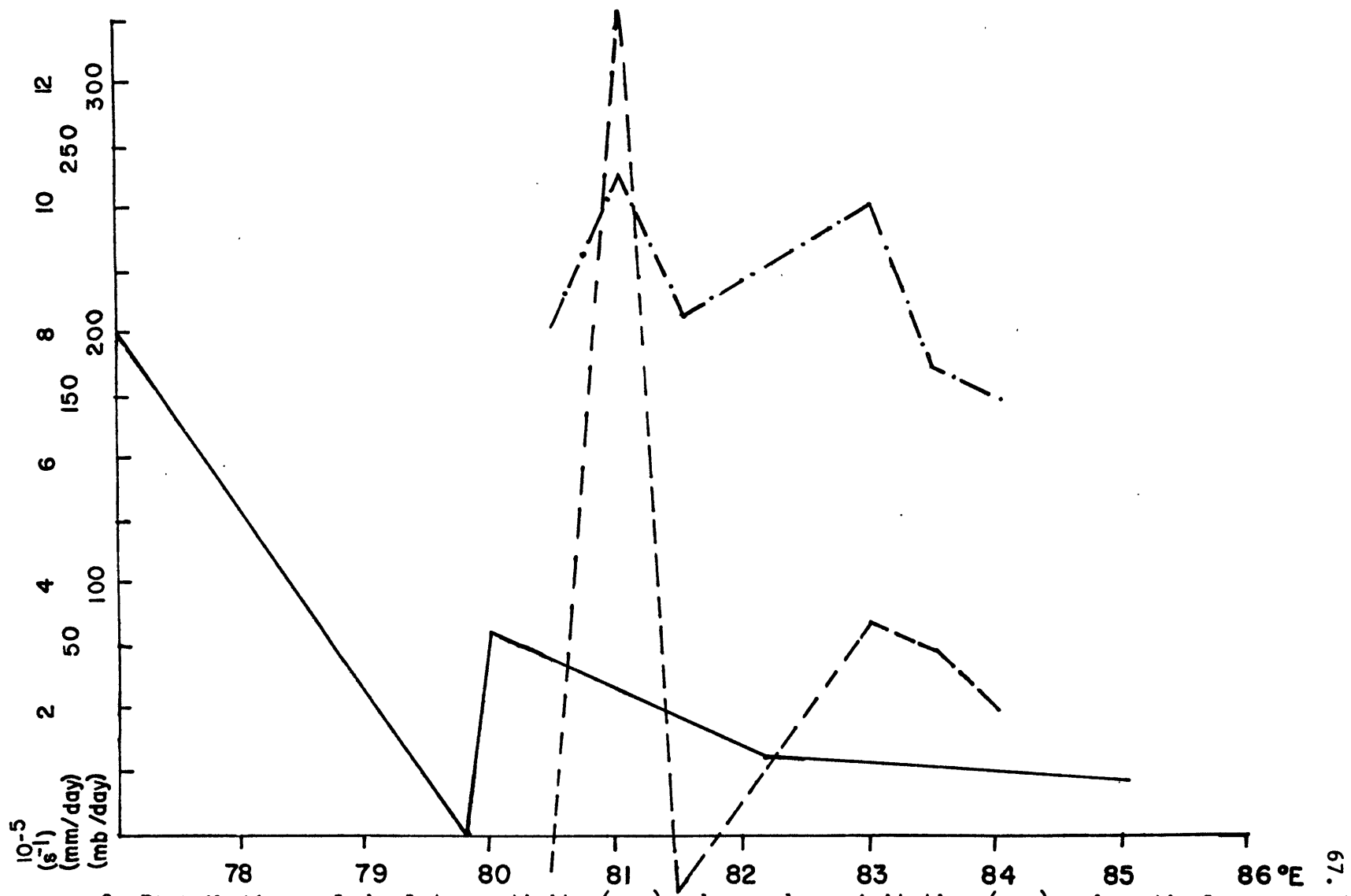

Figure 38. Distributions of absolute vorticity (—·—), observed precipitation (——) and vertical velocities (– – –) calculated from the continuity equation around 23°N on 8-28-73 at 850 mb.

CHAPTER 5

Vertical Transport Processes

5.1 Definition of the Tropopause

The primary concern of this research is to study the vertical propagation of tropospheric constituents into the stratosphere. Our assumption was that a few well-developed synoptic events along the ITCZ each year may account for a large portion of the air masses exchanged across the tropopause.

Reiter states,

> ".... evidence leads us to the conclusion that the tropopause is a permeable 'membrane' through which large and small transport processes effect a continuous mixing between tropospheric and stratospheric air masses. For quantitative estimates of such processes it is important to define the exact location in space of this 'membrane'.

The tropopause is a transition between the troposphere and the stratosphere. Soundings usually show a sharp change in the lapse rate of temperature occurring between the tropopause and the nearly isothermal distribution of the stratosphere. This discontinuity usually denotes the tropopause. There are many ambiguities with this definition from station to station over a given area, thus, the "mean" tropopause level in our study is simply defined to coincide with the 100 mb surface.

5.2 Tropospheric - Stratospheric Mass Exchange

The processes responsible for stratospheric-tropospheric mass exchange are: 1) seasonal adjustment in the height of the tropopause; 2) organized large-scale quasi-horizontal and vertical motions expressed

by the mean meridional circulation; 3) large-scale eddy transports mainly in the jet stream region; and 5) mesoscale and small-scale eddy transport across the tropopause.

Reiter has estimated that an amount of air approximately 70% of the stratospheric mass is involved in stratospheric-tropospheric exchange each year. Seasonal changes of tropopause heights accounts for exchange of about 10% of the stratospheric mass each year. Vertical transport through the Hadley cell transfers approximately 38% of the mass, and large-scale eddies and anticyclones transfer about 20%. Approximately 1% was attributed to continuous small-scale and mesoscale vertical diffusion processes. Heck and Panofsky (1975) confirmed Reiter's results in their study of transport processes in the lower stratosphere.

Our objective is to quantify the impact of synoptic disturbances along the ITCZ on exchange processes. In order to estimate what effect the monsoon disturbances had on exchange mechanisms, mass balances were constructed over the depression. Vertical velocities were analyzed at the 100 mb level of the triangular areas investigated and the vertical mass flux Φ was computed using

$$\Phi = -\frac{\omega}{g} \tag{5.1}$$

where g is the acceleration due to gravity and ω is the vertical velocity at the 100 mb level.

In Table 2 we have summarized the 100 mb ω values computed in each triangle or quadrilateral. These ω values can be translated into mass fluxes (in kgm km^{-2} sec^{-1}) by multiplying by 1.02×10^{7} (cf.

Equation 5.1).

To give an idea of the upward mass transport possible during the three-day period which we have analyzed in detail, the mass flux was calculated for three small triangles in which upward vertical velocities are observed at the 100 mb level (Figures 24-26). The velocities were computed using Equation 3.4 over the triangles ABC, ACE and DEF. The fluxes of mass for these triangles were 6.3×10^2 $kgkm^{-2}$ s^{-1}, 1.4×10^3 $kgkm^{-2}$ s^{-1}, and 1.8×10^3 $kgkm^{-2}$ s^{-1} respectively. These triangles could transport a total of 7.5×10^{16} grams of air across the 100 mb level. This represents .2% of the total mass of the stratosphere.

A very rough estimate of the mass transported upwards through the 100 mb level over August the entire Summer Monsoon (June, July, August) and over the entire continental region of India can also be made using observed rainfall. Figures 39-41 show the observed precipitation in India during the months of June, July, and August respectively. There is heavy monsoon rain in southwestern and eastern India. The heaviest rainfall was to the east of India along the East Asian monsoon trough. The average monthly rainfall for the continental region was 18.7 cm, 39.4 cm, and 36.9 cm for the sequence of three months. The average rainfall for the northeastern and southwestern regions were 8.9 cm and 64.9 cm for June, 51.7 cm and 70.1 cm for July and 44.4 cm and 64.2 cm for August. Using Equation 3.4 and the vertical distribution of diabatic heating in Figure 19, Table 3 shows the average daily vertical velocity across the 100 mb level for the summer months. The maximum continental vertical velocity at the 100 mb level was 2.6×10^{-3} mbs^{-1} occurring in the month of July. The maximum vertical velocity for the northeastern

and southwestern regions also occurred in the month of July with values of 3.4×10^{-3} mbs^{-1} and 4.5×10^{-3} mbs^{-1} respectively.

We computed an upward flux of 2.0×10^{20} grams for the Indian region for the month of August. Reiter (1975) states that the total mass of the stratosphere is approximately 8.52×10^{20} grams. The mass flux of 2.0×10^{20} grams accomplished by the Indian region for the month of August therefore represents 25% of the total mass of the stratosphere. The velocities in Table 3 correspond to an average mass flux of 6.3×10^{4} $kgkm^{-2}$ s^{-1} for the Indian continent, 7.0×10^{4} $kgkm^{-2}$ s^{-1} for the northeastern region and 1.3×10^{4} $kgkm^{-2}$ s^{-1} grams for the southwestern region across the 100 mb surface over the three summer months. Of the total flux of the continental area 15% is attributed to the southwestern region and 34% to the northeastern region.

5.3 Vertical Flux of Fluorocarbons

A knowledge of troposphere-stratosphere exchange mechanisms is essential to an understanding of the physical basis for the vertical distribution of various stratospheric minor constituents. Here we attempt to quanitfy the distribution of the halogen species $CFCl_3$ and CF_2Cl_2.

The observed tropospheric mixing ratios are 2.40×10^{-10} $volvol^{-1}$/ 6.11×10^{-10} $kgkg^{-1}$ and 1.30×10^{-10} $volvol^{-1}$/7.78×10^{-10} $kgkg^{-1}$ respectively.

The flux of $CFCl_3$ and CF_2Cl_2 across the 100 mb level over the three days investigated was 2.0×10^{-5} $kgkm^{-2}$ s^{-1} and 2.6×10^{-5} $kgkm^{-2}$ s^{-1} respectively. The average flux of $CFCl_3$ over the continental area is 3.8×10^{-5} kgkm s^{-1} for the three month sequence. The average flux from the northeastern and southwestern regions is 4.3×10^{-5} $kgkm^{-2}$ s^{-1} and

7.9×10^{-6} respectively.

The average flux of CF_2Cl_2 over the continental area is 4.9×10^{-5} $kgkm^{-2}$ s^{-1} $\times 10^{-1}$ g/s for the three months and the average flux from the northeastern and soutwestern regions is 5.4×10^{-5} $kgkm^{-2}$ s^{-1} and 1.0×10^{-5} $kgkm^{-2}$ s^{-1} respectively. These values are obtained by using Equation 3.4 and the diabatic distribution of heating from Yanai. These values represent an area of 9.5×10^{5} km^2 for the northeastern region and 3.0×10^{5} km^2 for the southwestern region.

The flux of $CFCl_3$ and CF_2Cl_2 across the 100 mb level is 1.5×10^{-4} $kgkm^{-2}$ s^{-1} and 1.9×10^{-4} $kgkm^{-2}$ s^{-1} respectively using the maximum vertical velocity obtained by Equation 3.6.

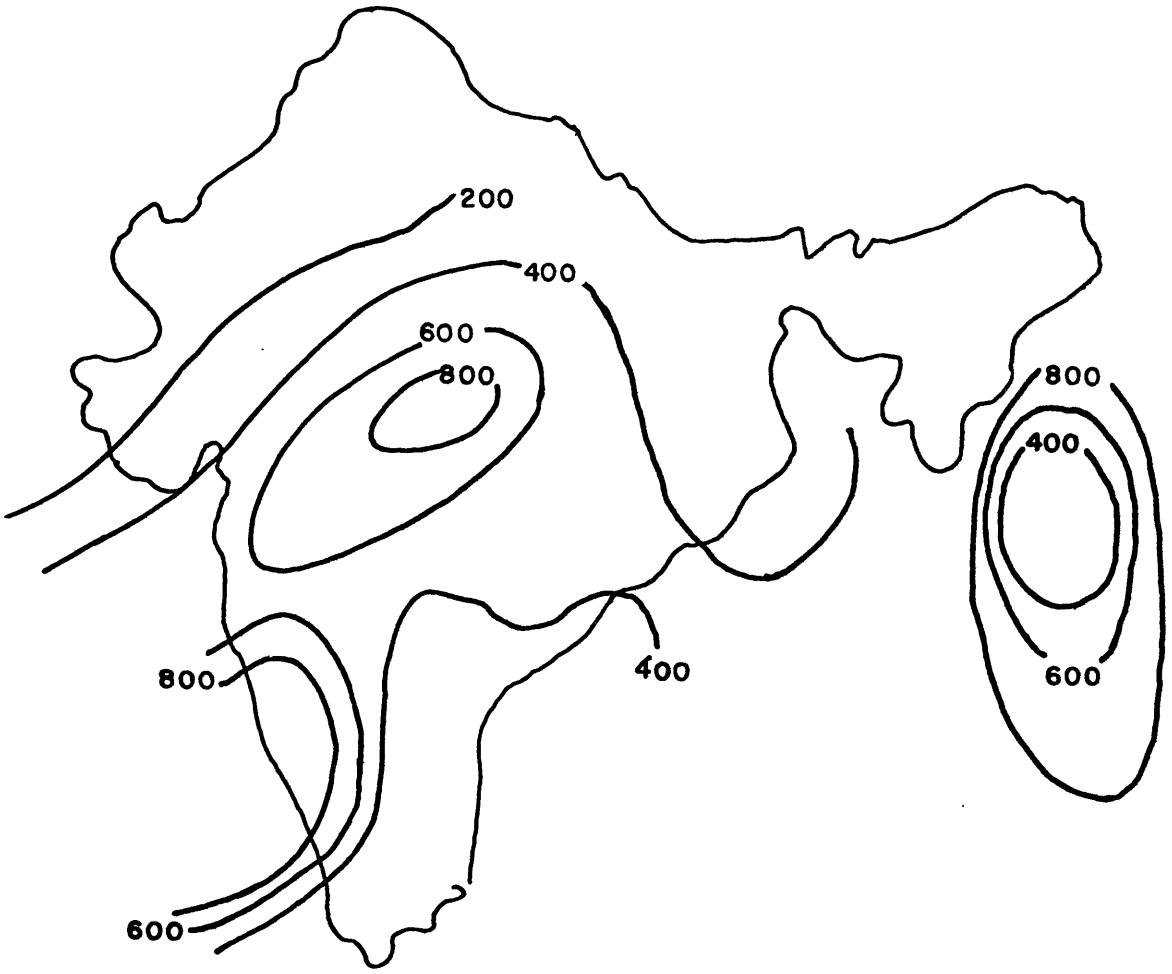

Figure 39. Observed precipitation (mm) for India during June, 1973.

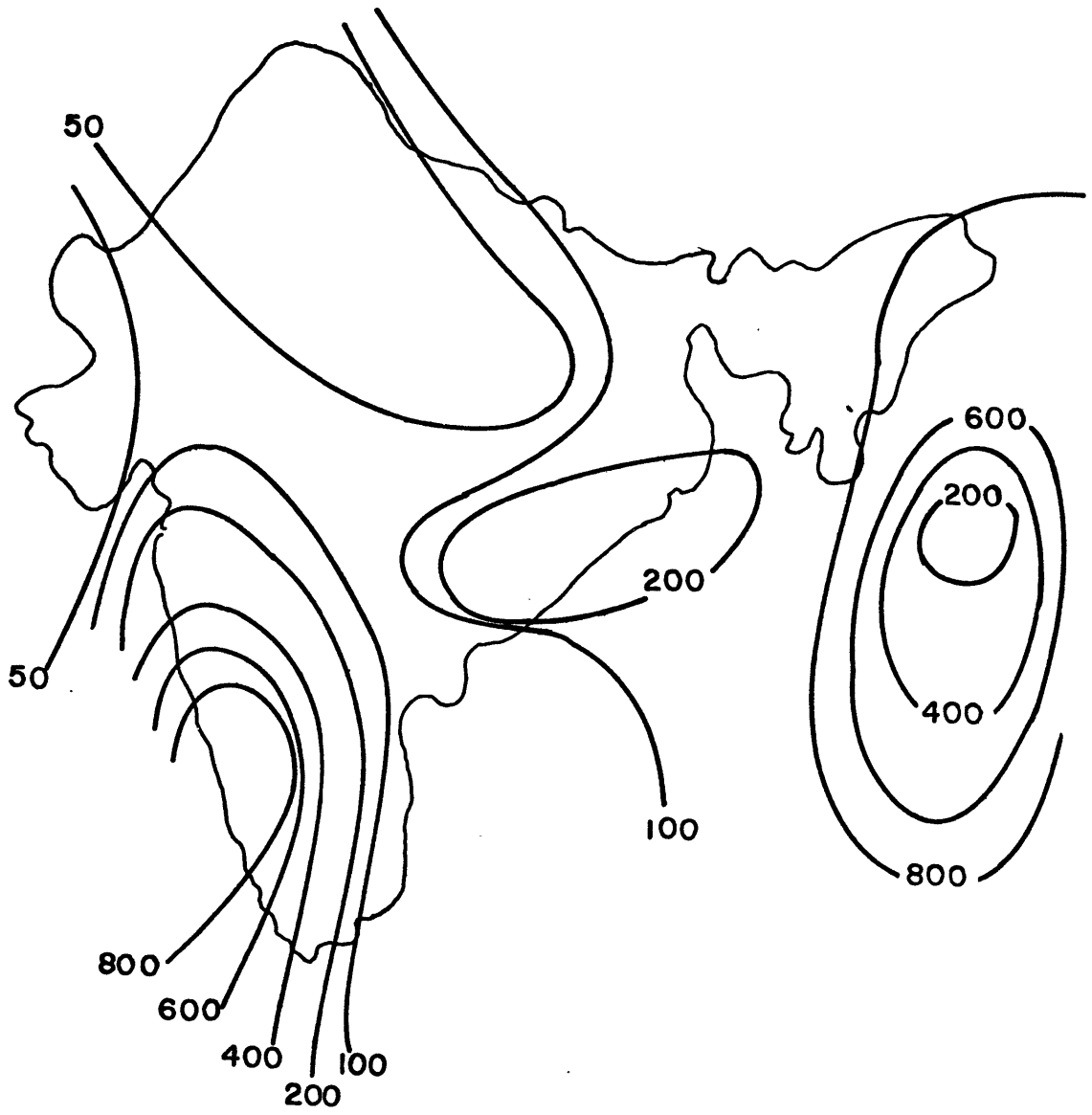

Figure 40. Observed precipitation (mm) for India during July, 1973.

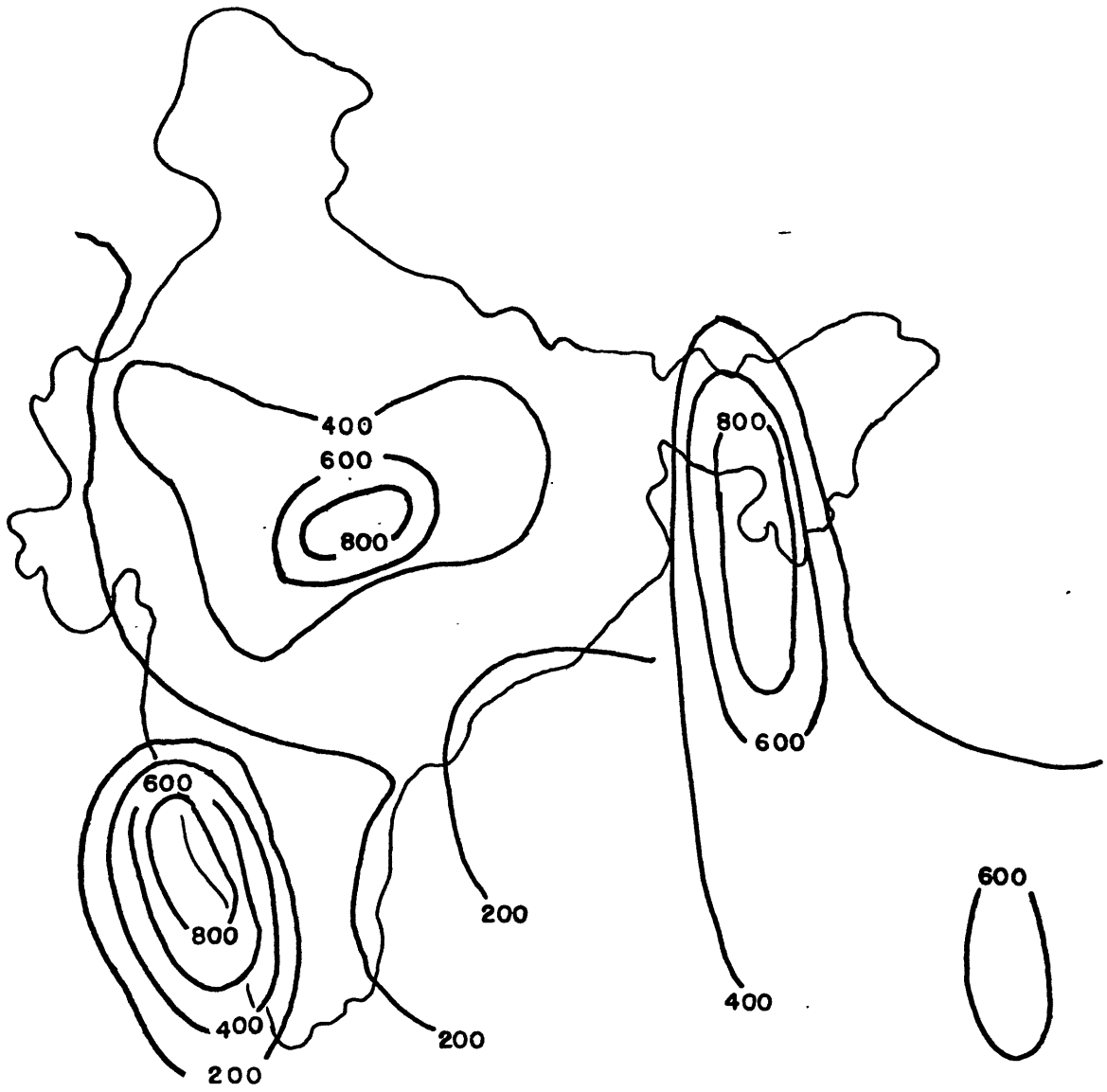

Figure 41. Observed precipitation (mm) for India during August, 1973.

TABLE 2

AREA	METHOD 1 10^{-3}mbs^{-1}			METHOD 2 10^{-3}mbs^{-1}			METHOD 3 10^{-3}mbs^{-1}		
	8/26	8/27	8/28	8/26	8/27	8/28	8/26	8/27	8/28
ΔDEF		1.1	-.3	-8.1	5.4	-10	-5.	-4.	-5.
ΔCEF		-.1	-5	12	-5.8	-18			
ΔCDE		-.5	-15	1.3	14	0			
ΔGIJ		-1.0	-.4	-14	-7	-3.7			
$\square$ GHIJ							-10	-8	-12
ΔABC							-5	-2	-3
Δ ACE							-2	-3	-7

Vertical velocities across the 100 mb level calculated from the adiabatic thermodynamic equation (Method 1), the continuity equation, (Method 2), and the diabatic thermodynamic equation (Method 3). These ω values can be translated into mass fluxes (kgkm^{-2}s^{-1}) by multiplying by 1.02×10^{7}.

TABLE 3

	CONTINENTAL AREA (10^{-3} mbs^{-1})	N.E. AREA (10^{-3}mbs^{-1})	S.W. AREA (10^{-3}mbs^{-1})
JUNE	1.2	.58	4.1
JULY	2.6	3.4	4.5
AUGUST	2.4	2.9	4.1

Vertical velocities across the 100 mb level calculated from the diabatic thermodynamic equation, Eqn. 3.4, in India for the month of August.

CHAPTER 6

Discussion and Conclusions

The present study was devoted to the Indian Summer Monsoon (June - August). From the result of a comparison of the continuity equation and the first law of thermodynamics, we found that the adiabatic thermodynamic equation neglecting diabatic heating was not valid below 400 mb. Saha (1966) found cloud tops and thus possible latent heating extending even above the 400 mb level over the land in the tropical regions. To assess latent heat releases the vertical distribution of non-radiative diabatic heating deduced by Yanai (1973) was used to determine the heating profile of the rainfall distribution observed. This enabled us to more reliably determine the vertical velocities of the intermediate levels between the cloud tops and the ground.

Mass fluxes obtained by the kinematic method were larger than those obtained by the adiabatic thermodynamic equation. We have considered the kinematic values as an upper limit and the adiabatic thermodynamic values as a lower limit at the upper levels. We were cognizant o f the fact that errors accumulate in the vertical with the use of the continuity equation; whereas with the adiabatic thermodynamic equation the static stability ($\partial\theta/\partial p$) calculated was a 24-hour average. Therefore the values obtained may be overestimates of the local temperature changes induced by forced ascent. In addition, latent heating is ignored. When latent heating was included in an approximate form of the diabatic thermodynamic equation velocities one to two orders of magnitude greater were obtained. Finally, in all three methods, because

condensation occurs primarily through cumulus convection, the vertical velocity must be that of the individual cumulus updrafts, not the synoptic vertical velocity. In most of the areas investigated the majority of the precipitation accumuluated within a six-hour period. Thus the vertical velocities calculated will be an average of the updraft and smaller velocities occurring outside of the immediate area; consequently, an underestimated value.

Net upward motion was observed over the Indian continent with large vertical motion over the northeastern and southwestern regions. The largest rainfall and therefore presumably the largest vertical velocities occurred during the month of July with only a slight decrease in magnitude for the month of August.

We found a direct correlation between the distributions of absolute vorticity, rainfall and vertical velocities.

Table 2 summarizes the different methods by which vertical velocities were calculated in this study across the 100 mb level. The adiabatic thermodynamic equation and the continuity equation were used to calculate vertical velocities for the triangular areas illustrated in Figures 7 and 8 over the three days, August 26 - August 28, 1973. The diabatic thermodynamic equation was used to calculate average vertical velocities in the northeastern region over the three days at the 100 mb level.

The average monthly mass flux was calculated from the monthly rainfall data for the Indian region. We computed an upward flux of 2.0×10^{20} grams which corresponds to 25% of the mass of the stratosphere for the Indian region for the month of August.

We also calculated an average mass flux of 6.3×10^4 $kgkm^{-2}$ s^{-1} using Equation 3.4 for the Indian continent over the three summer months (June - August, 1973). The mass input of 5.2×10^{20} grams accomplished by the Indian region for the three months represents 61% of the total mass of the stratosphere.

There have been a few measurements made of the $CFCl_3$ and CF_2Cl_2 content of the troposphere and stratosphere. The average fluxes of $CFCl_3$ and CF_2Cl_2 across the 100 mb level calculated in our study were 1.5×10^{-5} $kgkm^{-2}$ s^{-1} and 1.8×10^{-5} $kgkm^{-2}$ s^{-1} respectively for the continental Indian region for the month of August. The estimated world production of $CFCl_3$ and CF_2Cl_2 in 1974 was 304×10^9 grams/year and 305×10^9 grams/year respectively (Rowland and Molina, 1975). Thus, the Indian region alone could possibly inject 39.5% of these fluorocarbons into the stratosphere. All mass fluxes quoted above reflect the use of the Yanai distribution and Equation 3.4.

The kinematic vertical velocities are probably invalid above the 400 mb level, thus the mass flux is not quoted for these. The vertical velocities obtained by the use of the Yanai distribution and Equation 3.4 appear to yield plausible estimates of the vertical motion in the monsoon region. The inherent assumption in using the Yanai distribution is that the high clouds found over the inland area of India extend well above the 400 mb level to approximately the 200 mb level. Thus the latent heating term in the full thermodynamic equation is assumed to be important even at the highest levels.

REFERENCES

Bellamy, J.C. (1949): Objective calculations of divergence, vertical velocity, and vorticity. Bull. Amer. Meteor. Soc., 30, 45-49.

Byers, H.R. (1974): General Meteorology. McGraw-Hill Book Co., Fourth Edition.

Danielson, E.F. (1968): Stratospheric-tropospheric exchange based on radioactivity, ozone and potential vorticity. J. Atmos. Sci., 25, 3, 502-518.

Holton, J.R. (1972): An Introduction to Dynamic Meteorology. Academic Press, N.Y.

Houze, R.A., Jr. (1973): A climatological study of vertical transport by cumulus-scale convection. J. Atmos. Sci., 30.

Krishnamurti, T.N. and R.J. Hawkins (1970): Mid-tropospheric cyclones of the southwest monsoons. J. Appl. Meteor., 9, 442-458.

Krishnamurti, T.N. and H.N. Bhalme (1976): Oscillations of a monsoon system, Part I. Observational aspects. J. Meteor. Soc. Japan, 33, 1937-1954.

Krishnamurti, T.N., et al. (1975): Study of a monsoon depression (I), synoptic structure. J. Meteor. Soc. Japan, 53, 227-240.

Krishnamurti, T.N., et al. (1976): Study of a monsoon depression (II), dynamical structure. J. Meteor. Soc. Japan, 54, 208-225.

Krishnamurti, T.N. (1971b): Observational study of the tropical upper tropospheric motion field during the Northern Hemisphere summer. J. Appl. Meteor., 10, 1066-1096.

Madden, R.A., and F.E. Rolutaille (1970): A comparison of the equivalent potential temperature and the static energy. J. Atmos. Sci., 27, 327-329.

Mahlman, J.D. (1964a): Relation of stratospheric-tropospheric mass exchange mechanisms to surface radioactivity peaks. Arch. Meteor. Geophys. Bioclimatol. A, 15, 1-25.

Ramage, C.S. (1971): Monsoon Meteorology. Academic Press, N.Y.

Ras, K.V. and S. Rajamani (1972): Study of heat sources and sinks and the generation of available potential energy in the Indian Region during the Soutwest Monsoon Season. Mon. Wea. Rev., 100, 383-388.

Reiter, E.R., M.E. Glasser, and S.D. Mahlman (1969): The role of the tropopause in stratospheric-tropospheric exchange processes. Pure Appl. Geophys., 12, 2, 185-218.

Reiter, E.R. (1975): Stratospheric-tropospheric exchange process. Rev. Geophysics and Space Physics, 13, 4, 459-474.

Saha, K (1968): On the instantaneous distribution of vertical velocity in the monsoon field and structure of the monsoon circulation. Tellus, 4, 601-619.

Schmeltekopf, A.L., et al. (1975): Measurements of stratospheric $CFCl_3$, CF_2Cl_2, and N_2O. Geophys. Res. Lett., 2, 9, 393-396.

Staley, D.O. (1962): Evaluation of potential vorticity changes near the tropopause and the related vertical motions, vertical advection of vorticity, and transfer of radioactive debris from stratosphere to troposphere. J. Atmos. Sci., 19, 6, 450-467.

U.S. Environmental Data Service, Monthly Climatic Data for the World. (1973), No. 26.

Yanai, E. and Chu (1973): Determination of bulk properties of tropical cloud clusters from large-scale heat and moisture budgets. J. Atmos. Sci., 30, 611-627.

Yau, M.K. (1973): A kinematic model to study the distribution of precipitation in a cumulus updraft. Masters of Science Thesis, Department of Meteorology, Massachusetts Institute of Technology.